shown in Figure 77 through 78.

The distribution of resistivity high corresponded to the Triassic systems agreed with that of low residual gravity. The feature stands in contradiction to the characteristics of the Triassic dolomite indicating high density and high resistivity in the laboratory test. In consideration that The Triassic systems lie on relative steep slopes, it is supposed that porous sands and mud lie between dolomites and unsaturated zone extends in the Triassic systems. This resistivity high overthrusts on the resistivity low in the plain area. This feature of the resistivity distribution corresponded to the geological structure such as the Triassic systems extend over the Cretaceous and the Tertiary systems.

The weak chargeability anomalies are recognized in the mineral occurrences except for the Bazina Kebira mineral occurrence. In the consideration that the mineralized specimens indicate high chargeability in the laboratory test, it is supposed that chargeability is the good parameter of mineralization in the survey area. Chargeability exceeding 5 mV/V is estimated around the H'Zamel Assoued mineral occurrence and the Koudiat Soda working. The relative high chargeability are located in the vicinity of the resistivity discontinuity running in the NE-SW direction, which corresponded to the boundary between the northwest resistivity high and the southeast resistivity low. Complicated geology such as the triple contact of the Triassic, the Cretaceous and the Tertiary around the Koudiat Soda working is reflected the complicated distribution of resistivity and residual gravity. The gravity distribution around the H'Zamel Assoued mineral occurrence same as that around Bou K'hil working and high chargeability exceeding 5mV/V within the relative high residual gravity and high resistivity

1.3.3 Siliana Prospect

(1) General Geology

The summary geological plan of Siliana prospect are shown in Figure 79 respectively. The stratigraphy comprises, in its ascending order, the Triassic system, the Barremian, Aptien and Albien formations of the Cretaceous system, the Eocene and Oligocene formations of the Palaeogene sub-system, the Miocene and Pliocene formations of the Neogene subsystem and the Quaternary system. The Triassic system directly contacts with the Cretaceous system with a sudden change in rock facies, lacking the Jurassic system between the two in the surface outcrops. The lower and middle Miocene formations are also lacking in the Neogene subsystem.

The Triassic system, distributing in the northeastern to central part of the prospect, consists of varicolored gypsum, limestone, pitch-black dolomite, and alternations of white

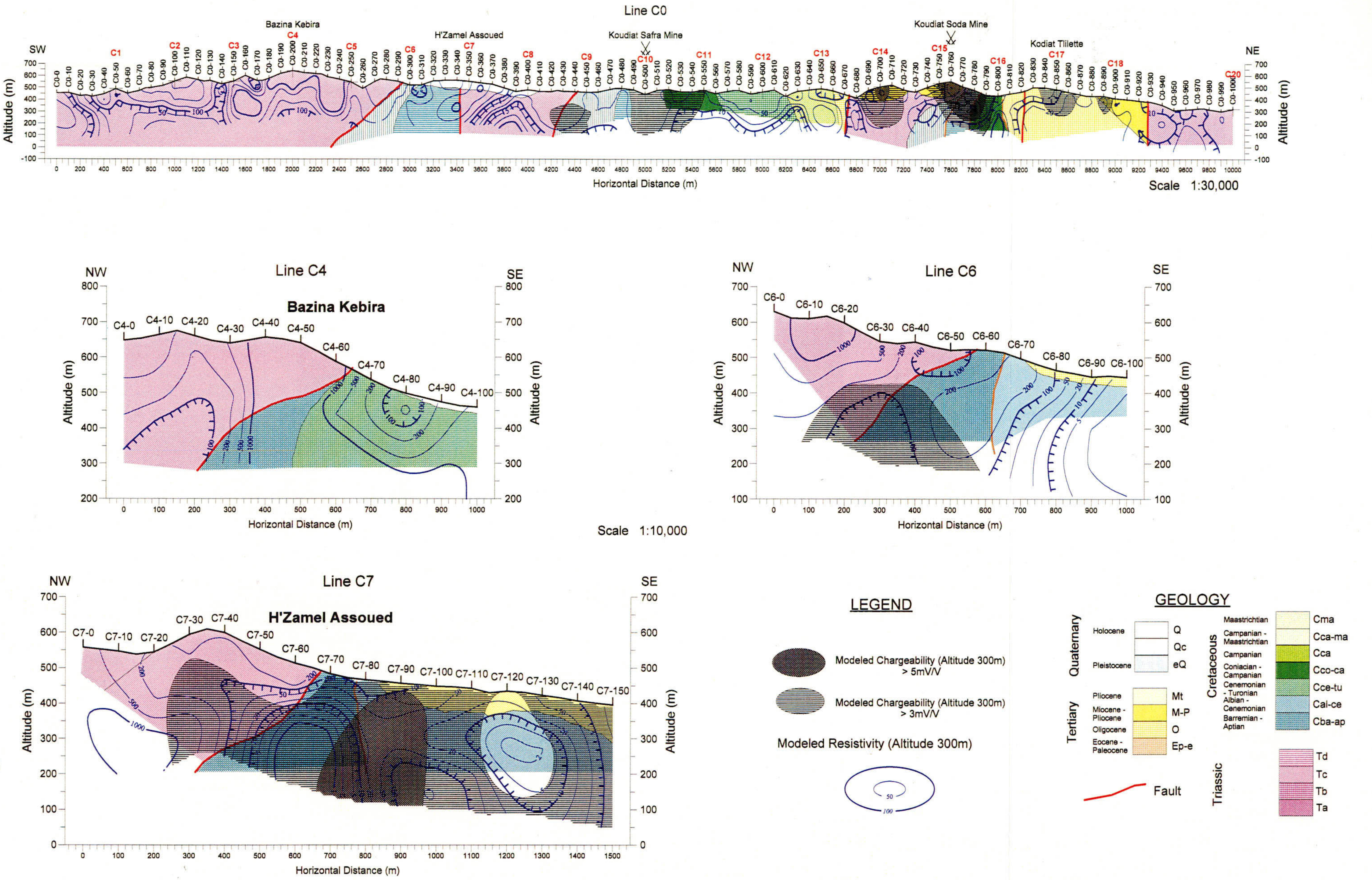

Figure 77 Interpreted IP Section (Line C0, C4, C6, C7)

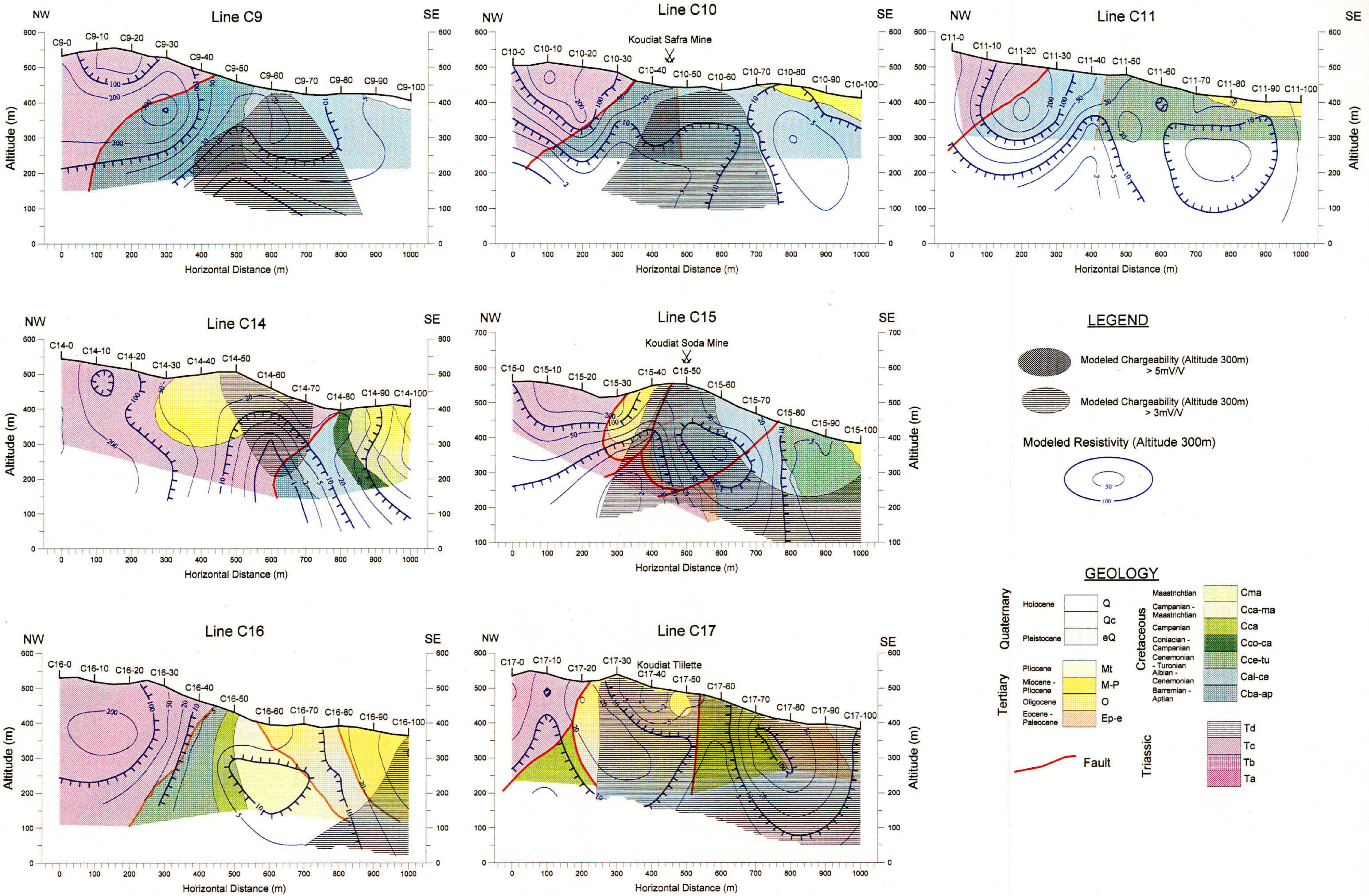

Scale 1:10,000

Figure 78 Interpreted IP Section (Line C9, C10, C11, C14, C15, C16, C17)

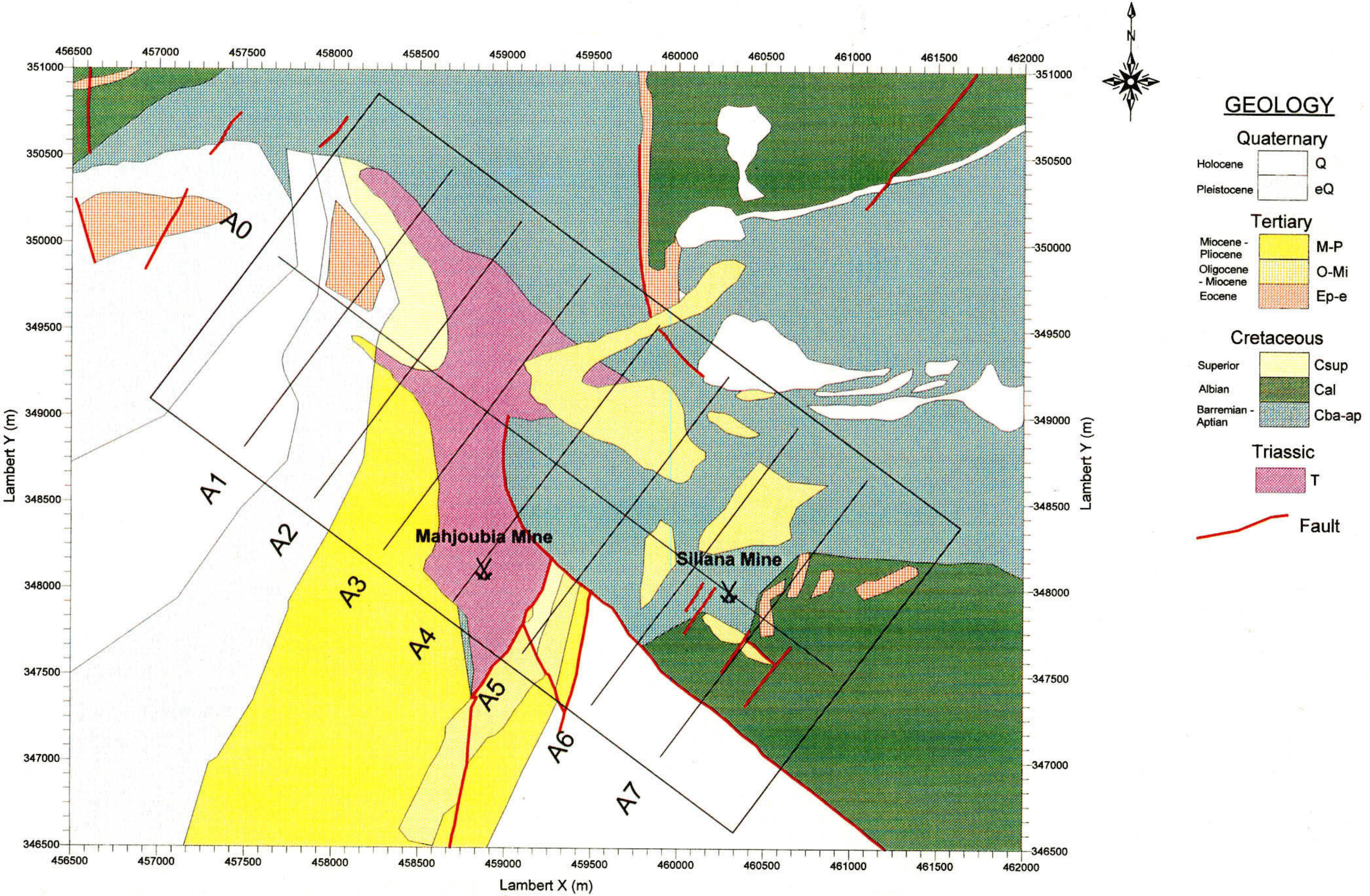

Figure 79 Geological map in Siliana prospect

sandstone and green argillite. Smoky quartz occasionally occurs in association.

The Barremian of the Cretaceous system, as a whole, forms an argillaceous limestone body in the northeastern corner that comprises gray to greenish marl and yellowish limestone. The Aptien, distributing in the central part, includes thin sandstone beds, sandstone-argillite alternations, green to olive marl and grayish argillaceous limestone. The thin sandstone beds and the sandstone-argillite alternations exhibit primary sedimentary structures indicating water-flow directions at the time of sedimentation. The argillaceous limestone often contains fossils of echinoderms. The Albien, distributing in the eastern part, principally comprises bluish gray marl showing spicular-fragmental appearances on outcrops and is occasionally interbedded with thin layers of limestone or argillaceous limestone.

The Eocene and Oligocene of the Palaeogene subsystem, distributing in the southern part and sporadically in the northwestern part, consist of alternations of thin marl layers and glauconitic limestone beds. The limestone beds form geomorphologically outstanding cliffs and contain silicified fossils of oysters, shark teeth and nummulites.

The Miocene and the Pliocene of the Neogene Tertiary extensively distribute in the western part of the prospect and consist of red sandstones, black marl, yellow to red siltstones and red conglomerates.

The Quaternary system includes pink-colored siltstones, brown conglomerates and chalky limestone containing bituminous materials.

The geologic structure of the prospect is characterized by diapirs and faults trending in the NNE-SSW direction and in the WNW-ESE direction. The diapirs, consisting of the Triassic formations, are mushroom-shaped with their umbrellas uniformly extending westwards from the stems and dipping reversely against the general trends of strata. The faults trending in the NNE-SSW direction divides the prospect into the northwestern and the southeastern parts. The northeastern part consists mainly of the Triassic diapirs and the Miocene-Pliocene formations of Neogene Tertiary. The southeastern part is further subdivided into two parts by the faults trending in the NNE-SSW direction; the one comprises the Cretaceous system and the other, the Tertiary and the Quaternary systems.

(2) Gravity Survey

① Regional Gravity Distribution (Figures 10 and 11)

The Siliana prospect is located at the southwestern side of an extensive rectangular area of the regional gravity high exceeding 10 mgal which is distributed to southeastward from the vicinity of the Lambert coordination (455,500,355,500) and is also situated on a saddle of the steep gravity gradient zone. The gravity decreases steeply towards an extensive gravity low in the El Aroussa plain spreading in the southern parts. A belt of the steep gravity gradient runs in the NW-SE direction, which suggests an existence of the regional geological structure.

② Gravity Distribution of the Prospect (Figure 80)

The belt of the steep gravity gradient extends uniformly towards the NW-SE direction on the regional gravity distribution. However the gravity contour intervals become narrower in the southern side of a line connecting the Mahjobia and Siliana workings and the direction of the gravity contours changes to the WNW-ESE direction. The gravity contours trend to be distorted in the vicinity of the line A4, which is running through the Mahjobia working and the geological structures are possibly different between the northwestern and southeastern sides divided by the line A4.

Both Mahjobia and Siliana workings are situated at the border of a change in pattern on the gravity distribution described above. The Mahjobia working is also situated at the boundary of the gravity distribution along the line A-4 and is considered to correspond to an intersection between two borders of different geological structures.

③ Residual Gravity Anomaly (Figure 81)

Six residual gravity anomalies are distributed in the prospect, two low anomalies below -0.2 mgal in the central and southern parts and four high anomalies exceeding 0.8 mgal surrounding the low anomalies. The low anomaly in the central parts extends towards northeast and is divided into two zones centering the stations A3-75 and A4-150 at the extremity of the anomaly. The low anomaly corresponds to an area where the Triassic dolomite with high density is distributed and therefore that is considered to suggest an existence of the other rocks with low density at depth. The low anomaly in the southern parts is situated in the northern margin of the El Aroussa plain covered by the unconsolidated layers of the Quaternary system. High anomaly extending towards the NE-SW direction through the Mahjobia working in the central parts of the prospect is characteristic among the high anomalies. The Siliana working is situated in the northwestern vicinity of small high anomaly, extending towards the NW-SE direction along the base line A0 in the southeastern parts of that. High anomaly is stretching towards east and west around the northeastern end of the line A1.

④ First Vertical Derivative Gravity Anomaly (Figure 82)

The positive zone of the first derivative gravity exceeding 0.005mgal/km extends from the central parts to the northern and eastern parts of the prospect. The negative zones are distributed in the southern and western parts. The 0mgal/km contours in the southern parts, which can be correlated to the faults and/or geological boundaries, are divided to three zones.

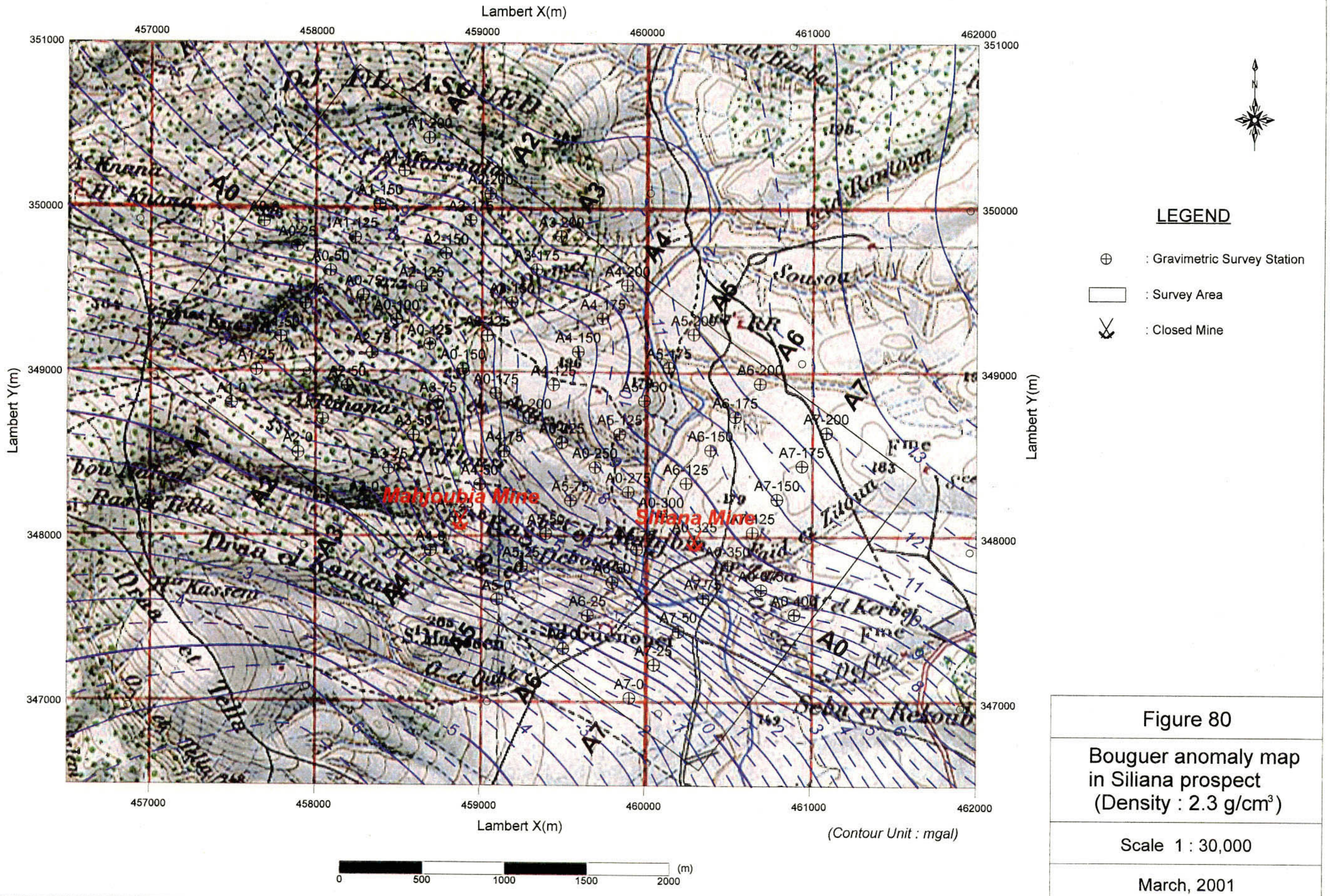

Figure 80

Bouguer anomaly map in Siliana prospect (Density : 2.3 g/cm^3)

Scale 1 : 30,000

March, 2001

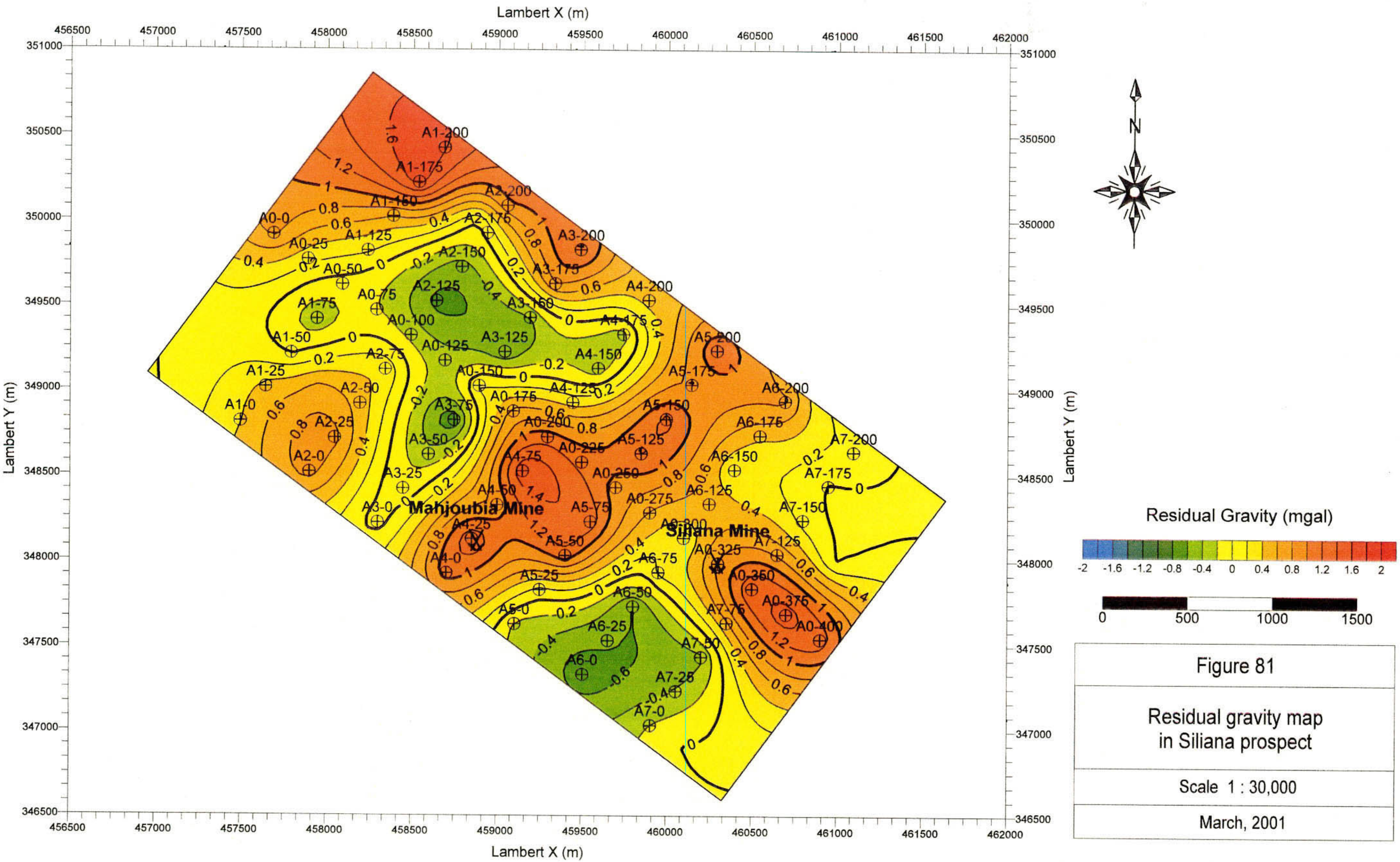

Figure 81

Residual gravity map
in Siliana prospect

Scale 1 : 30,000

March, 2001

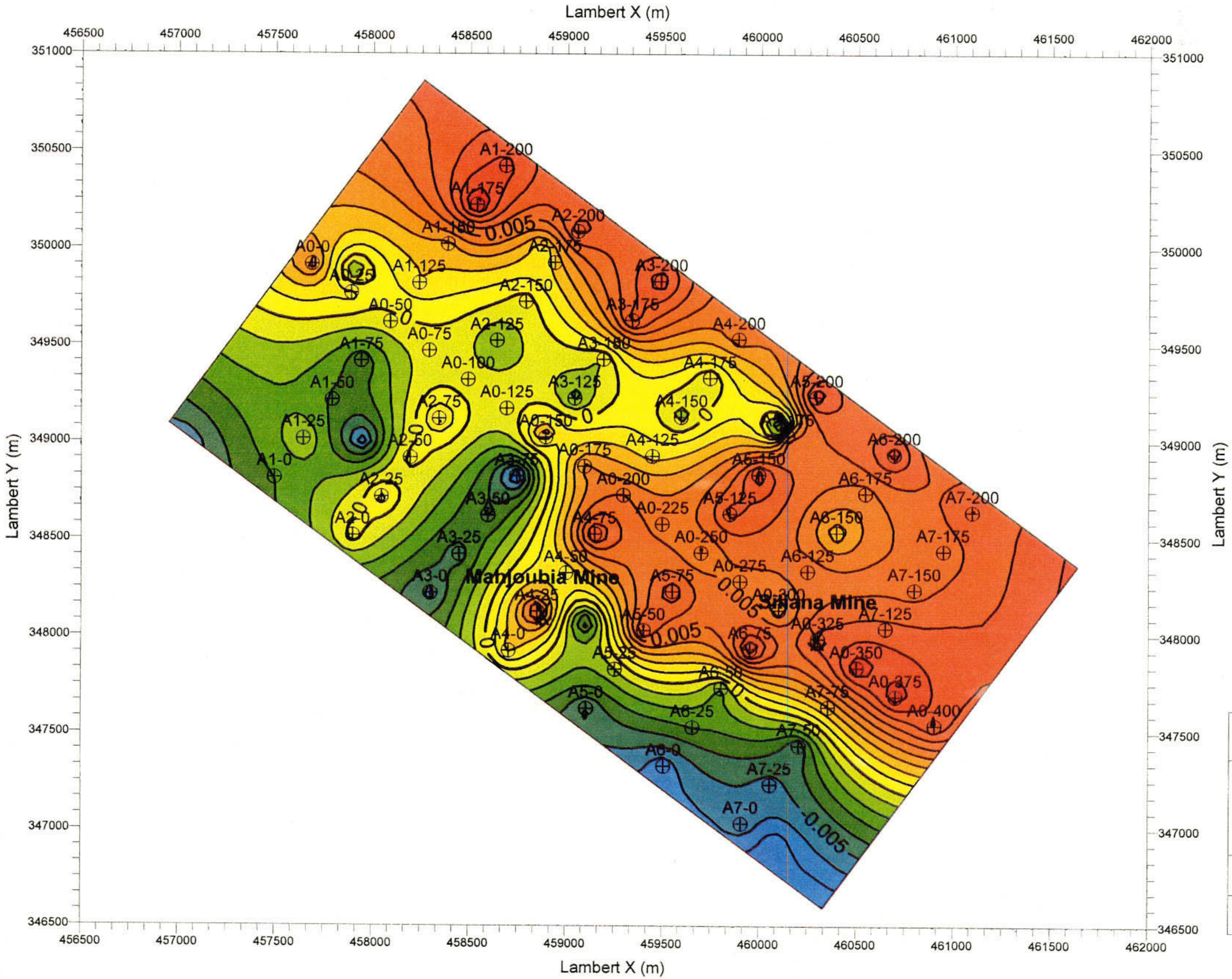

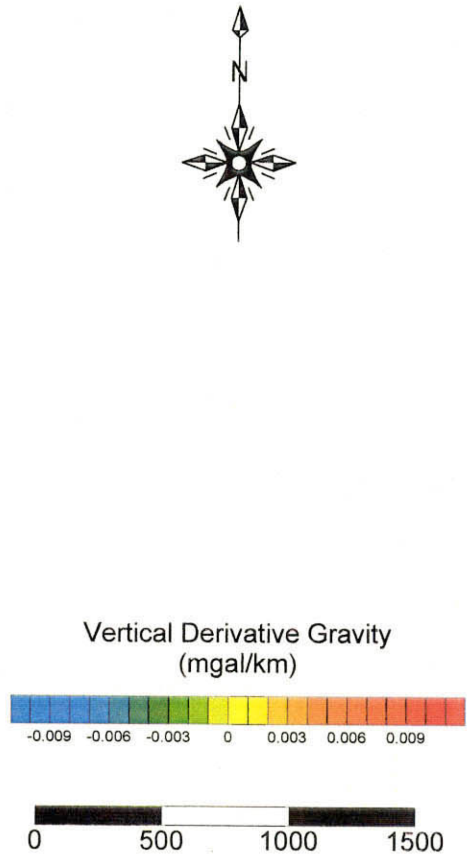

Figure 82

Vertical first derivative gravity map in Siliana prospect

Scale 1 : 30,000

March, 2001

The 0mgal/km contour in the northern parts is running generally towards west. The 0mgal/km contour in the central parts extends towards the NNE-SSW direction at the stations between A3-100 and A4-0, and crosscuts at the southern parts towards A7-50 in the east-southeastern parts. The general trends in first derivative gravity distribution are apparently different from that in the residual gravity anomaly. The locations of an individual anomaly are correlated with that of the residual gravity anomaly. The Mahjobia working is situated in a zone of small high anomalies aligned in along the NNE-SSW direction and the Siliana working is situated at the margin of high anomaly zone extending along the base line A0 in the eastern parts of the prospect.

⑤ Cross Section Analysis

The cross section analysis of the Siliana prospect is principally carried out assuming three layer's gravity structure and the depth of gravity model is determined. Those three layers are composed of the low density layers with density differences 0.10g/cm^3 of the Cretaceous system, -0.05g/cm^3 of the Tertiary system and/or -0.20g/cm^3 of the Quaternary system and the gravity basement with density difference of 0.00 g/cm^3 that is correlated to the Triassic system.

・ Cross Section A0 (Figure 83)

This is a longitudinal section crosscutting the prospect area from the northwestern parts to southeastern parts through the Siliana mineralized zone. The layer of high density with density difference of 0.01 g/cm^3 that is correlated to the Cretaceous limestone is dominated almost entirely in the cross section. The gravity basement, which is correlated to the Triassic system distributing between the stations A0-120 and 160, rises to near the surface, and both sides of the basement rise form the vertical structure similar to the fault. The surface is underlain by the low density layer with density difference of -0.05 g/cm^3 which may reflect the Tertiary system in the vicinity of the Siliana River running at the stations between A0-250 and A0-330 in the southeast parts of the cross section. The Siliana working is situated at southeastern parts of the layer with low density. The surface is widely covered by thin low density layer with density difference of -0.20 g/cm^3, which may reflect the Quaternary system.

・ Cross Section A1(Figure 84)

This cross section is running in the northwestern parts from southwest to northeast and the gravity structure is similar to that of the line A0. The layer with density difference of 0.01 g/cm^3 that is correlated to the Cretaceous limestone is dominated almost entirely in the cross section. The gravity basement, which is correlated to the Triassic system distributing in the

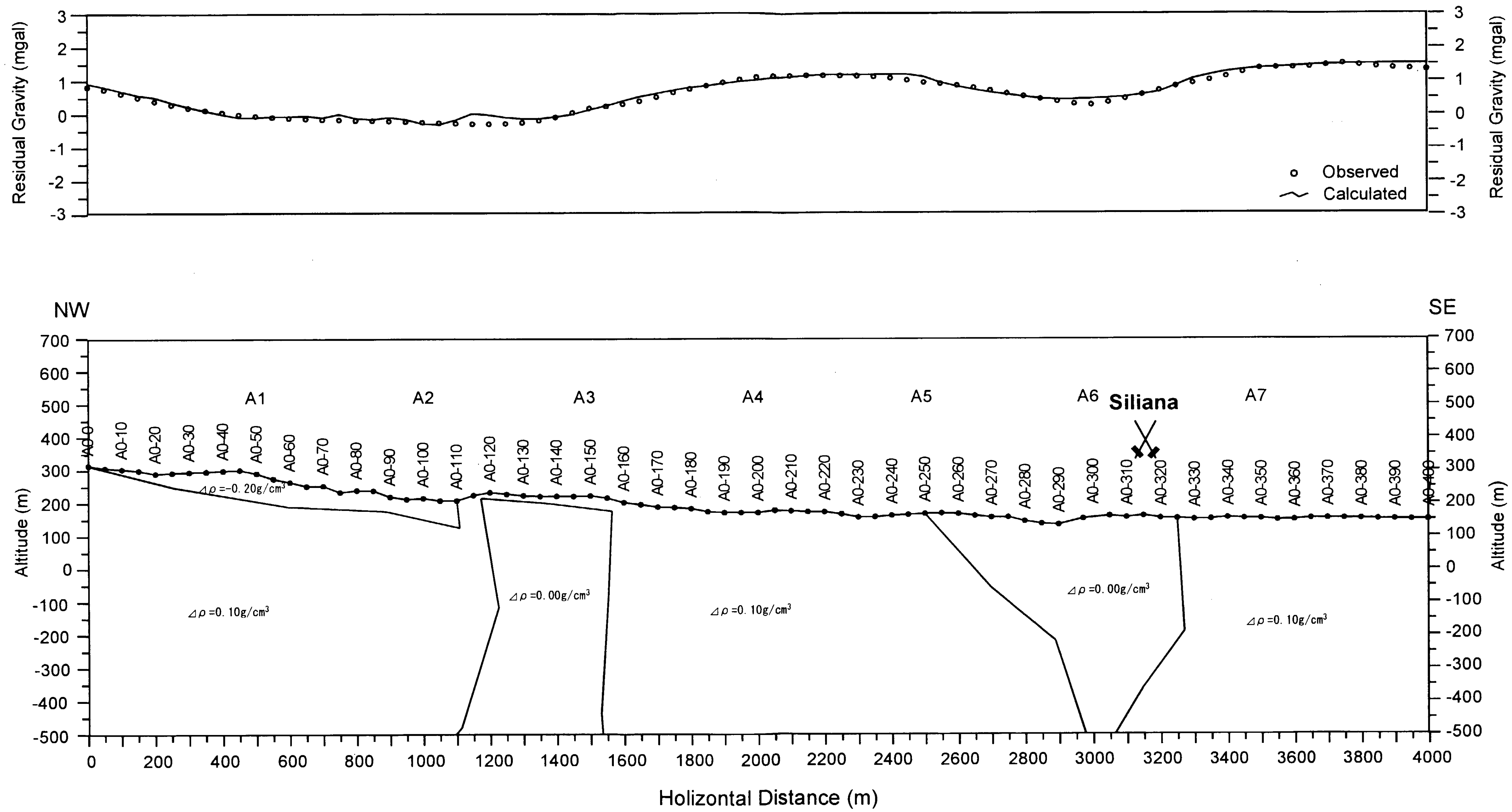

Figure 83
Result of 2-D Gravimetric analysis (Line A0)
Scale : 15,000
March, 2001

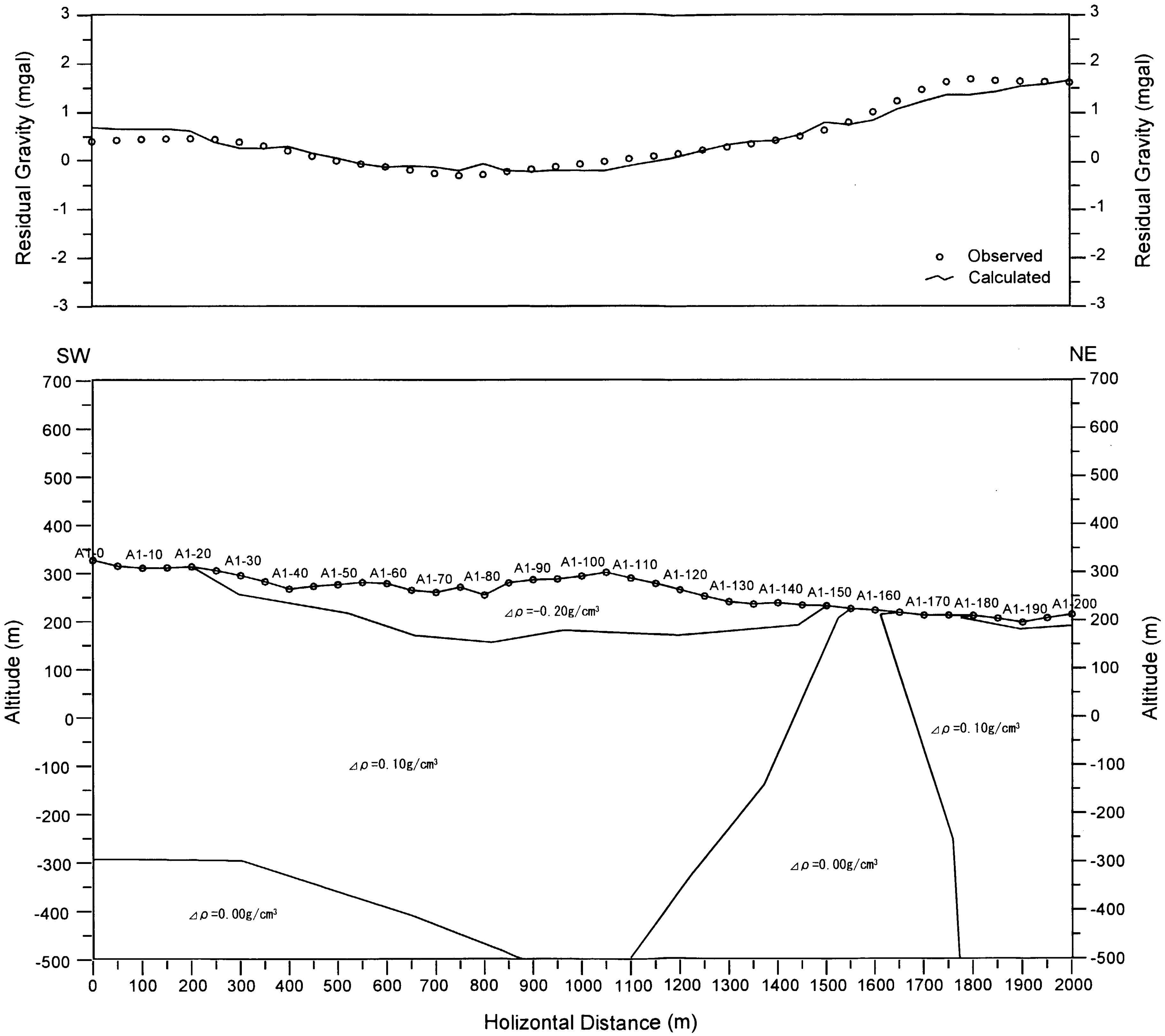

Figure 84
Result of 2-D Gravimetric analysis (Line A1)
Scale : 10,000
March, 2001

stations between A1-150 and A1- 160 in the central parts of the cross section, rises up to near the surface. Both sides of the basement rise contact with the Cretaceous system, especially the boundary of the northeastern side forms the vertical structure similar to the fault. The surface of the stations between A1-35 and A1-140 in the central parts is widely covered by thin low density layer, the thickness of which is ranging from 50m to 100m, and the density difference of that layer is-0.20 g/cm^3, that may reflect the Quaternary system.

・Cross Section A2 (Figure 85)

This section crosscuts in the NE-SW direction at 500m to the southeast from the cross section A1. The gravity structure is different from that of the cross section A1. The gravity basement correlated to the Triassic system extends almost entirely to the cross section. The high density layer with density difference of 0.01 g/cm^3, which is correlated to the Cretaceous system, is located at near the surface of the stations between A2-0 and A2-90 in the southwestern parts and in the northeastern end of the cross section. The surface of the stations between A2-100 and A2-180 and between the stations A2-45 and A-90 in the central parts is widely covered by thin low density layer with density difference of -0.20 g/cm^3, which may reflect the Quaternary system.

・ Cross Section A3 (Figure 86)

This section crosscuts in the NE-SW direction at 500m to the southwest from the cross section A2. The gravity structure is similar to that of the cross section A2. The gravity basement that is correlated to the Triassic system extends at the stations between A3-50 and A3-160 in the central parts of the cross section. The high density layer with density difference of 0.01 g/cm^3 that is correlated to the Cretaceous system is located in the southwestern parts from the station A3-50 and in the northeastern parts from the station A3-160. The boundary between the gravity basement and the layer with high density shows the structure similar the fault. The high density layer with density difference of 0.20 g/cm^3 over the stations between A3-85 and A3-115 in the central parts of the cross section is distributed on the surface of the gravity basement that may indicate a distribution of the Triassic dolomite.

・Cross Section A4 (Figure 87)

This section crosscutting the central parts of the prospect in the NE-SW direction runs longitudinally through the Mahjobia deposit. The gravity basement that is correlated to the Triassic system rises to near the surface of the stations between A4-5 and A4-10, between A4-30 and A4-55 and between A4-125 and A4-180. The gravity basement distributed widely appears to divide the thick layer with density difference of 0.10 g/cm^3 that is correlated to the Cretaceous system. The boundary between the gravity basement and the layer with high

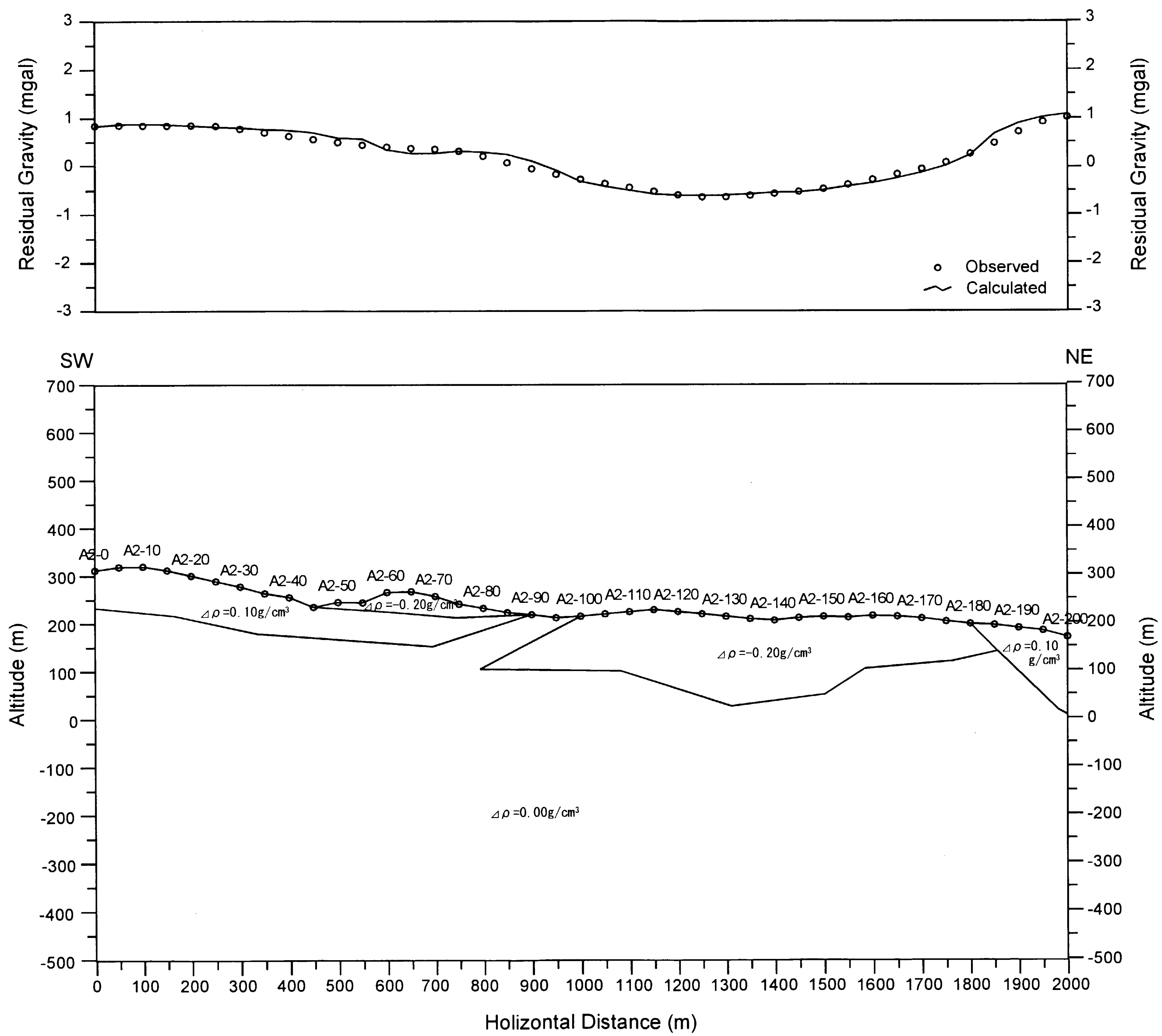

Figure 85
Result of 2-D Gravimetric analysis (Line A2)
Scale : 10,000
March, 2001

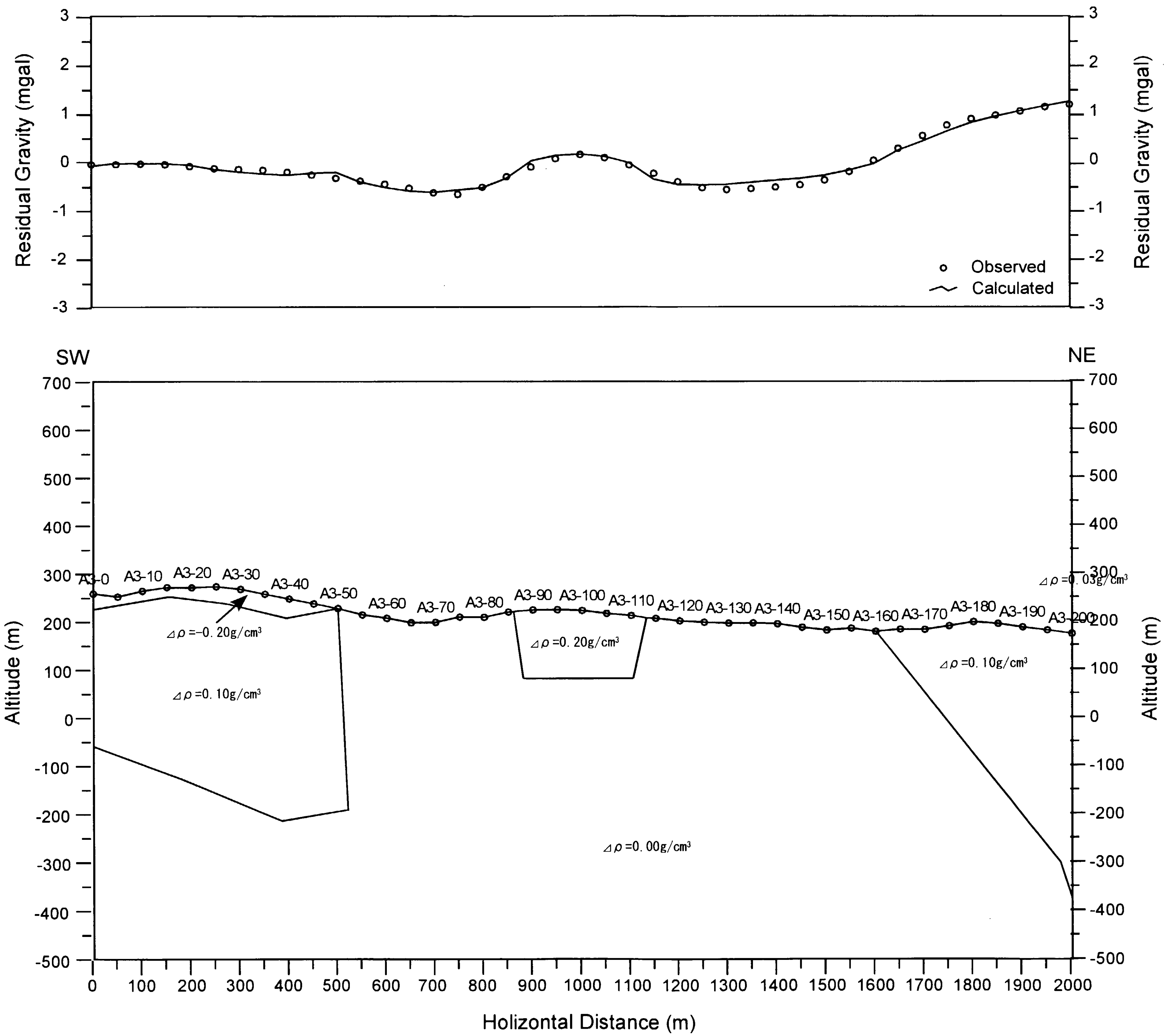

Figure 86
Result of 2-D Gravimetric analysis (Line A3)
Scale : 10,000
March, 2001

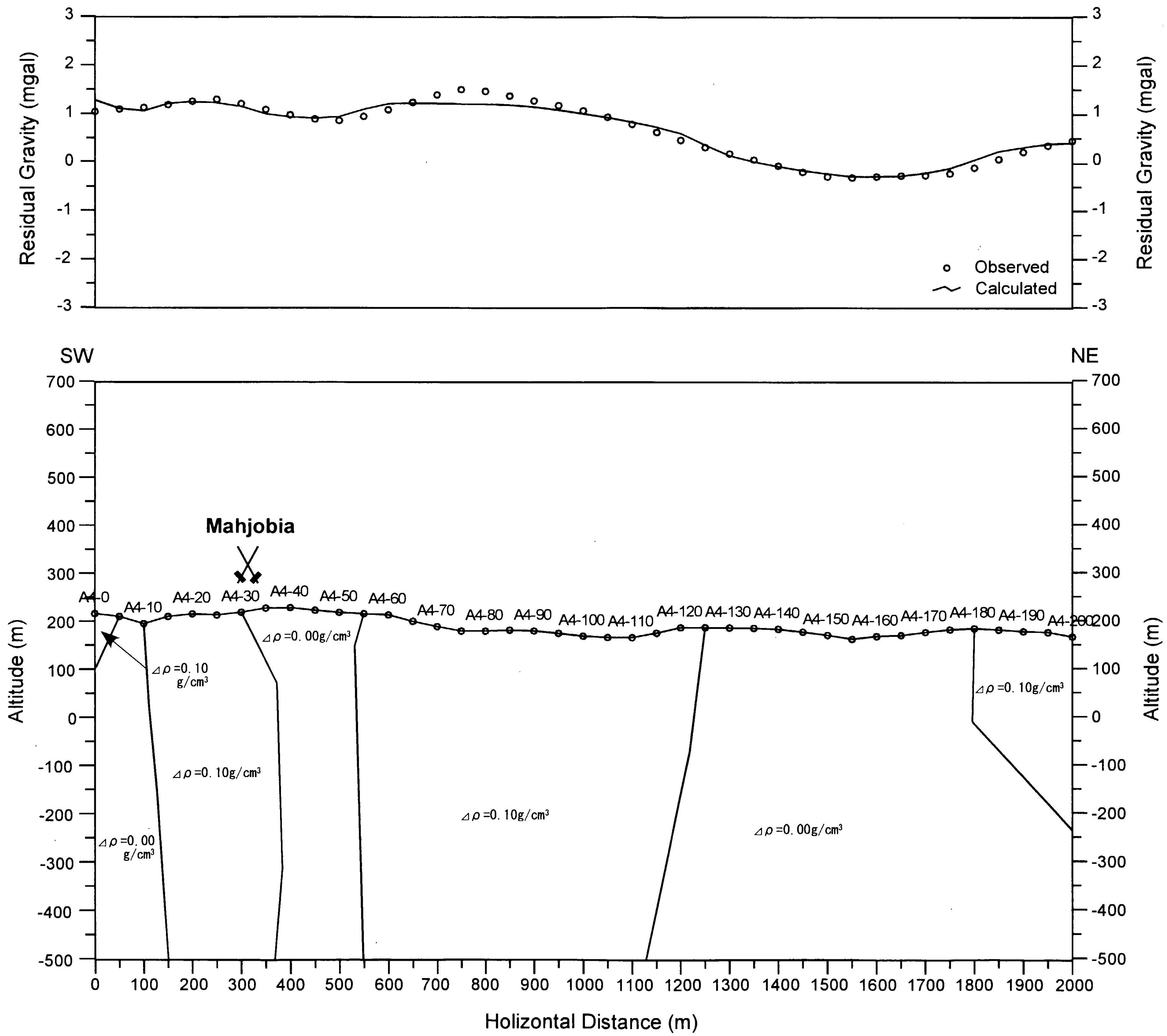

Figure 87

Result of 2-D Gravimetric analysis (Line A4)

Scale : 10,000

March, 2001

density suggests an existence of the fault. The Mahjobia working is situated at the border between the gravity basement and the layer with high density.

・Cross Section A5 (Figure 88)

This section crosscuts in the NE-SW direction at 500m to the southeast from the cross section A4. The surface layer of low density with density difference of -0.05 g/cm^3 correlated to the Tertiary system extends to the southwestward from station A5-50 and the surface layer of high density with density difference of -0.10 g/cm^3 correlated to the Cretaceous system extends to northeastward from station A5-50. Boundary of both layers forms the structure similar to the fault.

The gravity basement rises to about 100m below the surface of the stations between A5-80 and A5-110 in the central parts. The thin surface layer of low density with density difference of -0.20 g/cm^{3}correlated to the Quaternary system extends to the vicinity of the Siliana River in the northeastern end of the cross section.

・ Cross section A6 (Figure 89)

This section crosscuts in the NE-SW direction through the vicinity of the Siliana deposit at 500m to the southeast from the cross section A5. The same as the gravity distribution of the cross section A5, the low density layer with density difference of -0.05g/cm^3, correlated to the Tertiary system, extends towards southwest from the station A6-60 in the southwestern parts and the layer with density difference of 0.10 g/cm^3, correlated to the Cretaceous system, extends to near the surface in the northeastern parts of the cross section. Boundary of both layers forms the structure similar to the fault. The gravity basement correlated to the Triassic system rises to about 100m below the surface at the stations between A6-140 and A6-180 in the central parts of the cross section.

・ Cross section A7 (Figure 90)

This section crosscuts the southeastern parts of the prospect in NE-SW direction. The low density layer with density difference of -0.05 g/cm^3 correlated to the Tertiary system, the high density layer with density difference of -0.10 g/cm^3 correlated to the Cretaceous system and the gravity basement align from southwest to northeast. Each boundary at around the stations A7-40 and A7-150 forms the structure similar to the fault. The lower density layer with density difference -0.20 g/cm^{3}correlated to the Quaternary system overlies on the surface of the Cretaceous system at the stations between A7-40 and A7-80 in the vicinity of the Siliana River and increases the thickness towards the boundary between the Tertiary system.

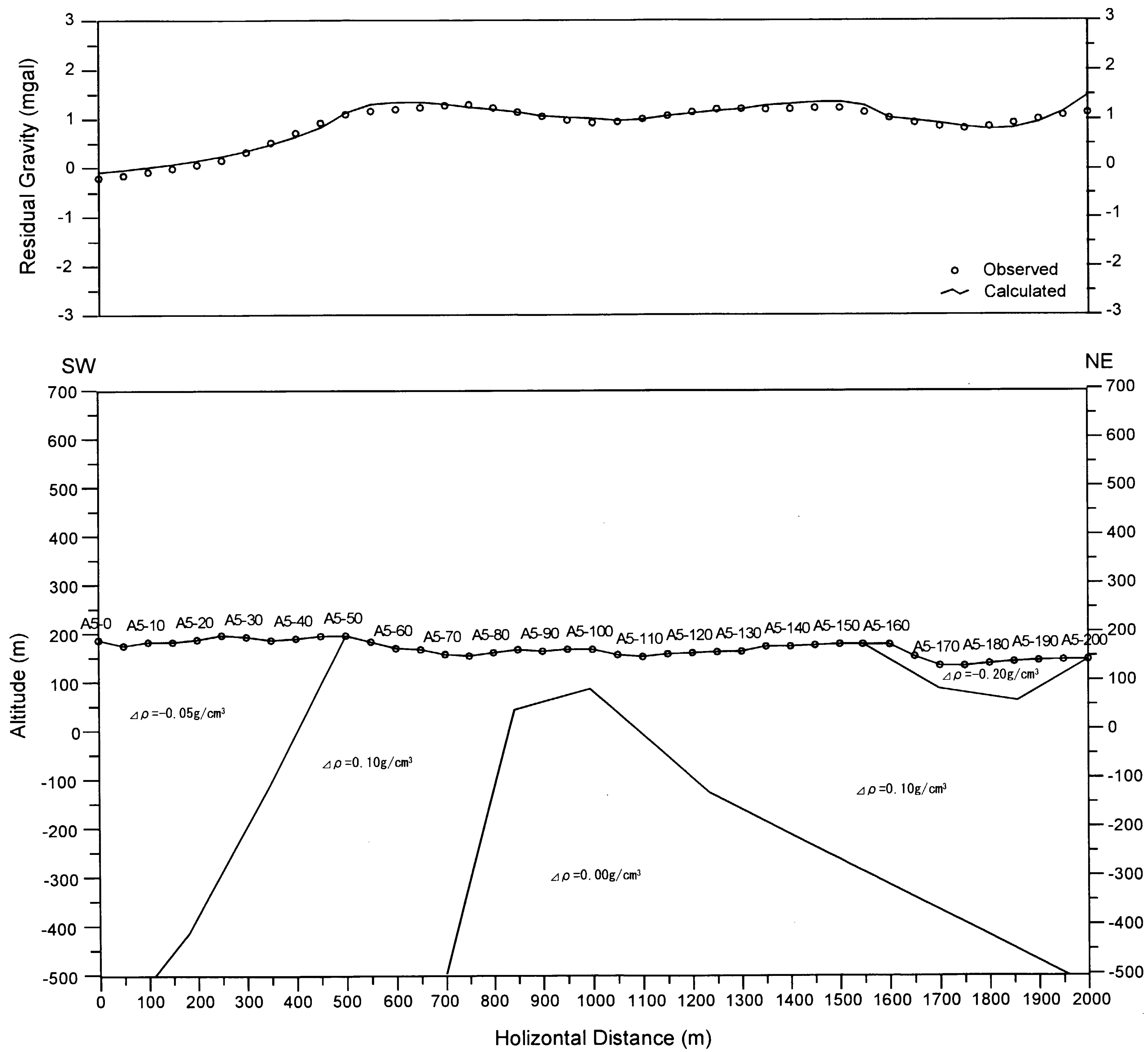

Figure 88
Result of 2-D Gravimetric analysis (Line A5)
Scale : 10,000
March, 2001

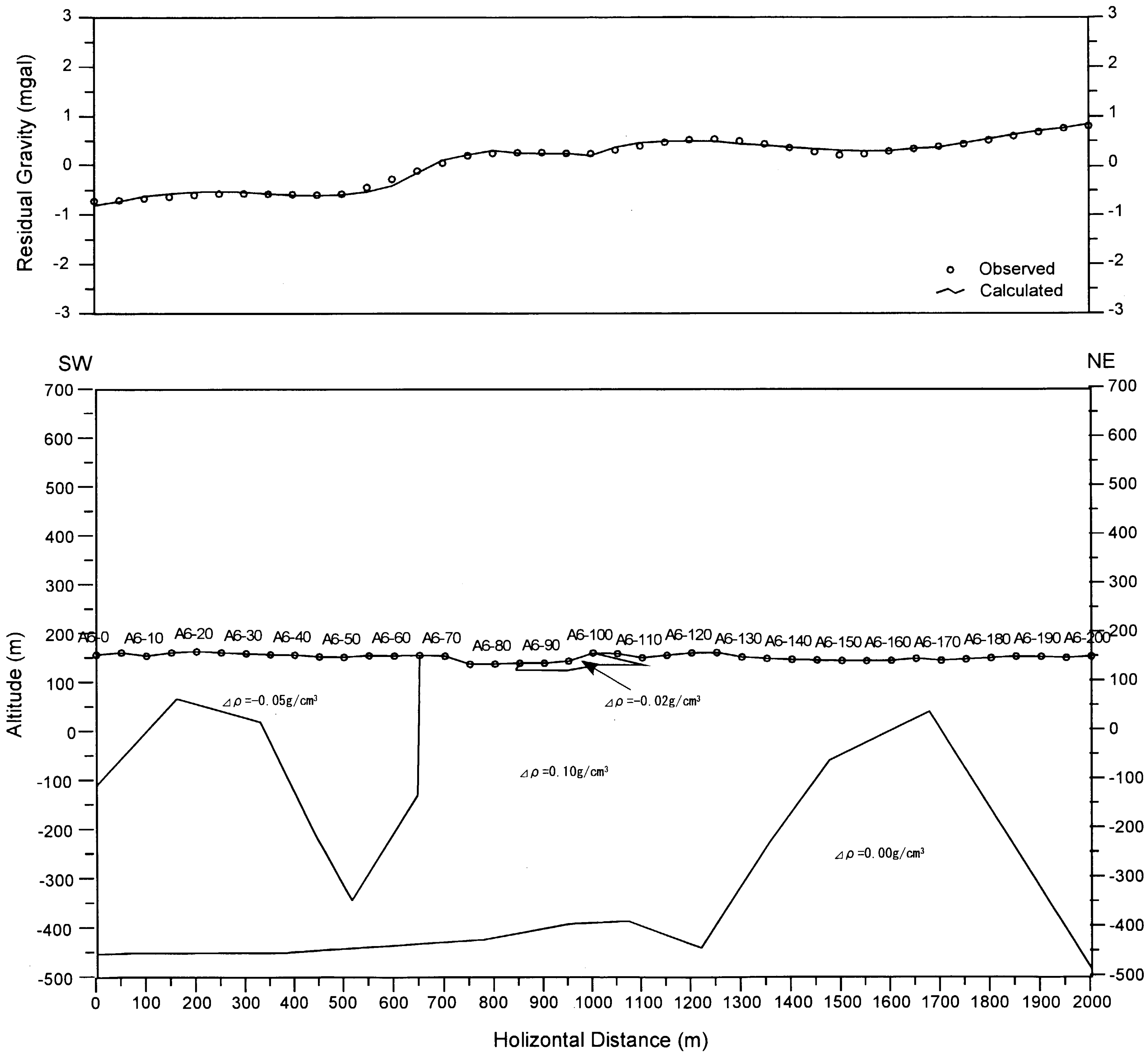

Figure 89
Result of 2-D Gravimetric analysis (Line A6)
Scale : 10,000
March, 2001

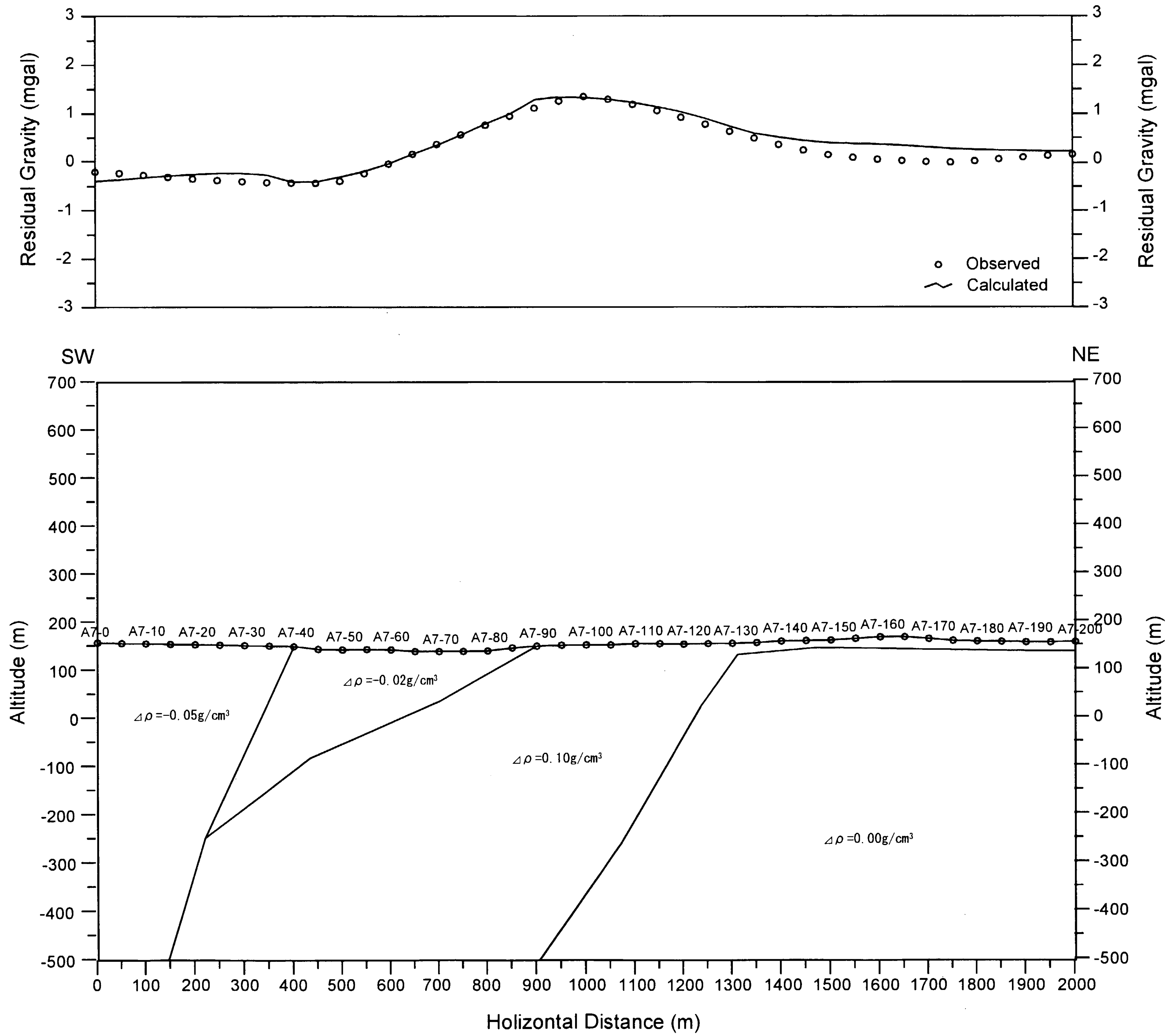

Figure 90
Result of 2-D Gravimetric analysis (Line A7)
Scale : 10,000
March, 2001

⑥ Interpretation of Gravity Plans

Characteristic residual gravity anomalies, the first vertical derivative gravity contours at 0 mgal/km and the Bouguer anomalies are superimposed over the geological map as shown in Gravity Interpretation Plan (Figure 91).

The smooth high gravity zones are distributed in the Cretaceous limestone area occurred at the northeastern parts of the prospect and the gravity values decrease gradually towards the Tertiary and Quaternary systems occur in the southwest parts. The belt of the steep gravity gradient extends along the fault in the NW-SE direction. This belt is shifted to the northern side along the eastern margin of the Triassic system, therefore it is suggested that the fault stretching from south-southwest to southwestern parts of the line A5 extends furthermore towards north-northeast. High residual gravity anomaly extends towards the NE-SW direction intersecting diagonally the blind fault mentioned above and the Mahjobia working is located in the southwestern margin of the residual gravity anomaly. High residual gravity anomaly extends from the southeastern to the northwestern parts along the baseline A0 in the southeastern parts of the prospect. The Siliana deposit is situated in the northwestern margin of the high residual gravity anomaly. The low gravity residual anomaly is correlated to the Triassic system occurring in the central parts of the prospect and the Triassic system is suggested to be the diapir with the low density the same as that of the Bazina Kebira prospect. The 0mgal/km contours in the southern parts can be correlated to the faults and/or geological boundaries run through from southeast to northwest generally along the fault in the prospect and extend to the northwestern parts where the Quaternary systems are distributed.

(3) IP Survey

①Apparent Resistivity and Measured Chargeability

Apparent rsistivity obtained in the prospect is ranging between 0.9 and 359 Ωm and an average is approximately 20 Ωm, which is rather low in general as compare with that of the Bazina Kebira prospect. The low apparent resistivities less than 10 Ωm are dominated in the southwestern side of the base line A0. The low apparent resitivity extends from the station A0-10 towards the station A1-130 in the western parts of the prospect and also extends towards the northern station A5-200 along the Siliana River in the central parts of the prospect. The southwestern side from the lines A6 and A7 correlates to the margin of the EL Aroussa plain covered by the Quaternary unconsolidated layer and also corresponds to the location of the low residual gravity anomaly. The high apparent resistivity zone exceeding 50 Ωm partially 100 Ωm extends towards the WNW-ESE direction in the northeastern side from

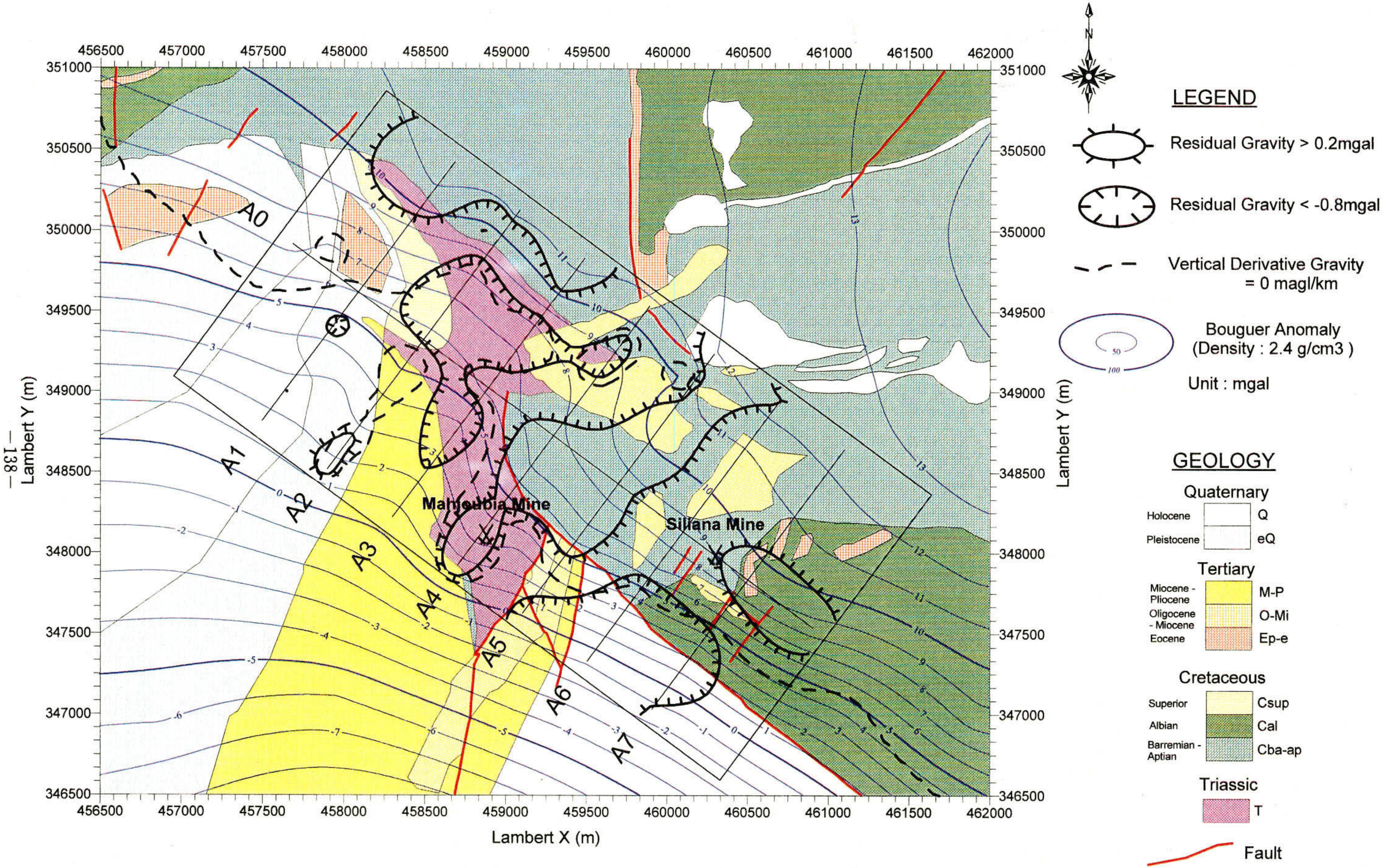

Figure 91 Gravity Interpretation Map in Siliana Prospect

the base line A0, covering the lines from A1 to A3 in the central parts of the prospect. The high apparent resistivity zone exceeding 50 Ωm is also dominated in the eastern parts of the prospect.

The distribution extent of both high and low apparent resistivity anomalies becomes wider according to an increasing electrode separation indices from n=1 to n=4 and the boundaries of those anomalies form a line of the resistivity discontinuity. Measured chargeabilities are low in general and show even maximum only 5.0 mV/V. The significant chargeability anomalies are not recognized except two weak anomalies exceeding 4 mV/V in the eastern parts of the prospect. Measured chargeabilities over the Mahjobia and Siliana deposits are also low.

Outlines of the resistivity and chargeability distribution recognized on the cross section, for the electrode separation indices n=1 through n= 4, are described below.

・Cross Section A0 (Figure 92)

This is a longitudinal section crosscutting the southeastern parts of the prospect through the Siliana deposit from the northwestern hill site to the southeastern plain area. The low apparent resistivity less than 20 Ωm is dominated in the entire cross section except the high apparent resistivity exceeding 100 Ωm, which is observed at the shallow depth of the stations between A0-130 and 160 in the central parts of the cross section. The low apparent resistivity anomalies below 10 Ωm are observed at the shallow depth of the northwestern parts, at the lower section of the high apparent resistivity anomaly and at depth of the section between the central and the southeastern parts of the cross section. The Siliana deposit is located at the northwestern margin of the high apparent resistivity anomaly exceeding 20 Ωm with thin thickness overlying the low apparent resistivity anomaly.

Measured chargeabilities are almost entirely weak in the cross section except a weak chargeability anomaly exceeding 4mV/V observed at 300m southeast from the Siliana working.

・Cross Section A1(Figure 93)

This cross section is running over the hill site in the northwest parts of the prospect from the southwest to the northeast. The low apparent resistivity less than 20 Ωm is widely distributed in the entire cross section. A low apparent resistivity anomaly less than 10 Ωm extends at shallow depth of the stations between A1-140 and A1-180 in the vicinity of the central parts of the cross section.

The significant chargeability anomaly is not recognized in this section.

・Cross Section A2 (Figure 94)

This cross section is running over the hill site at 500m to the southeast of the cross section

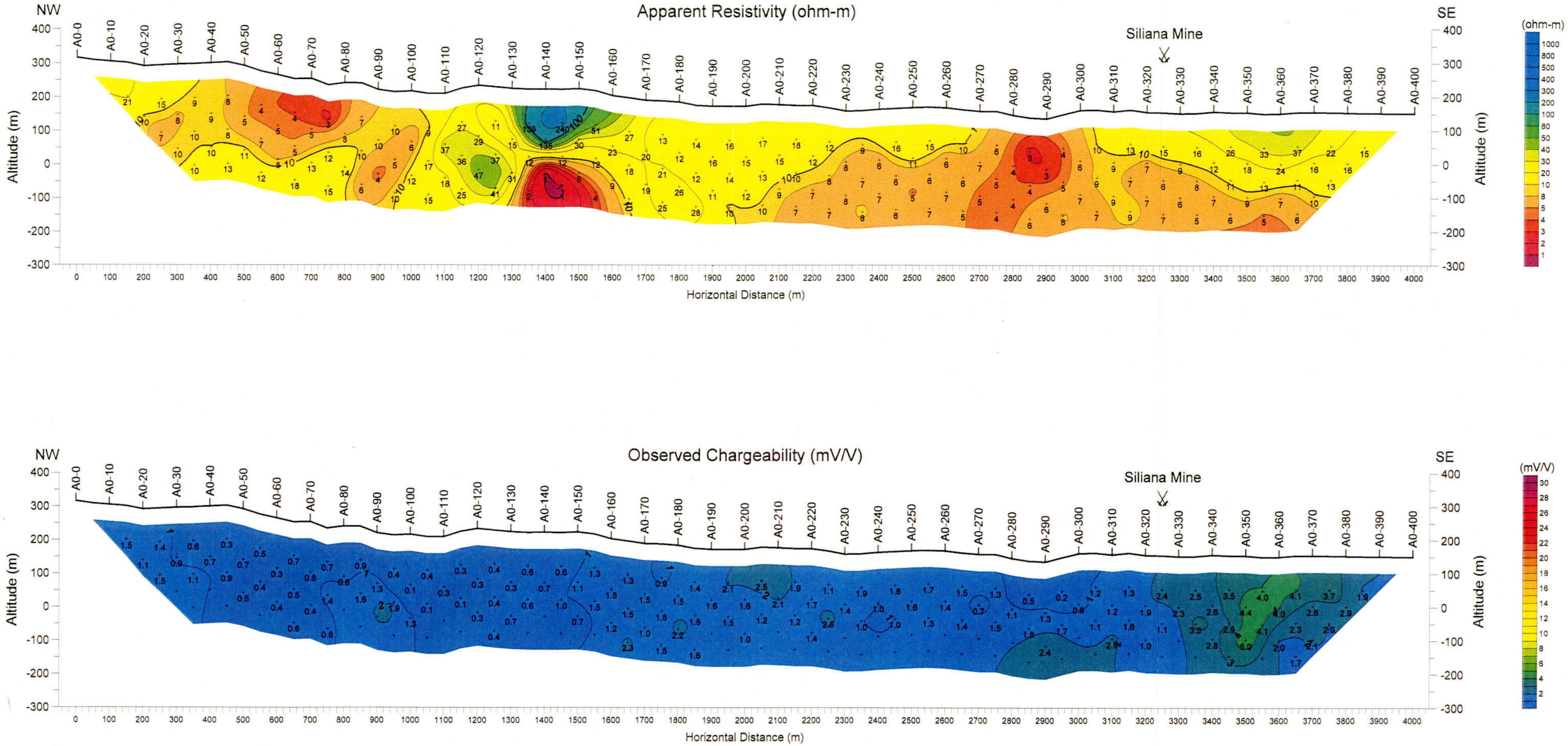

Figure 92 Observed IP pseudo-section (Line A0)

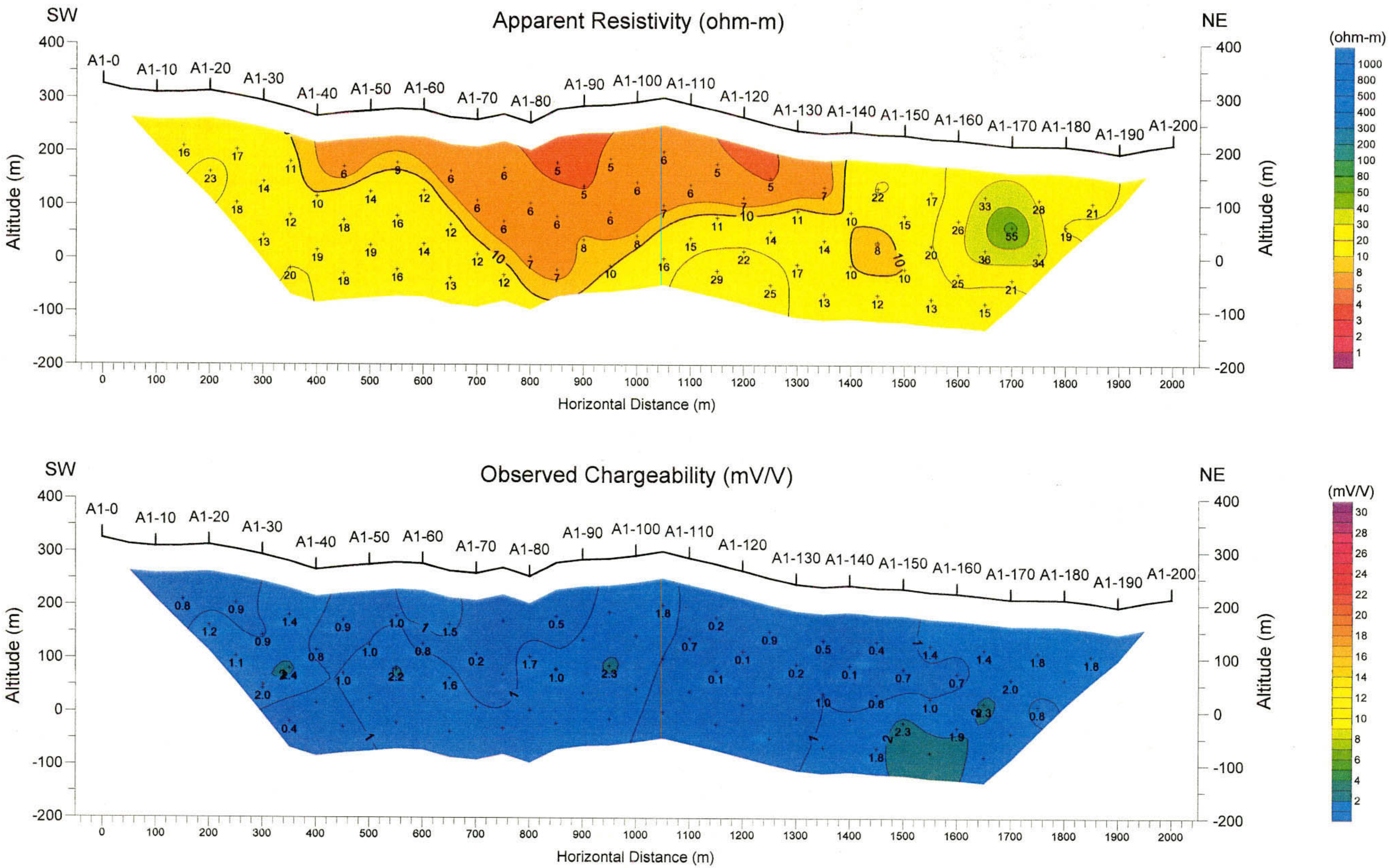

Figure 93 Observed IP pseudo-section (Line A1)

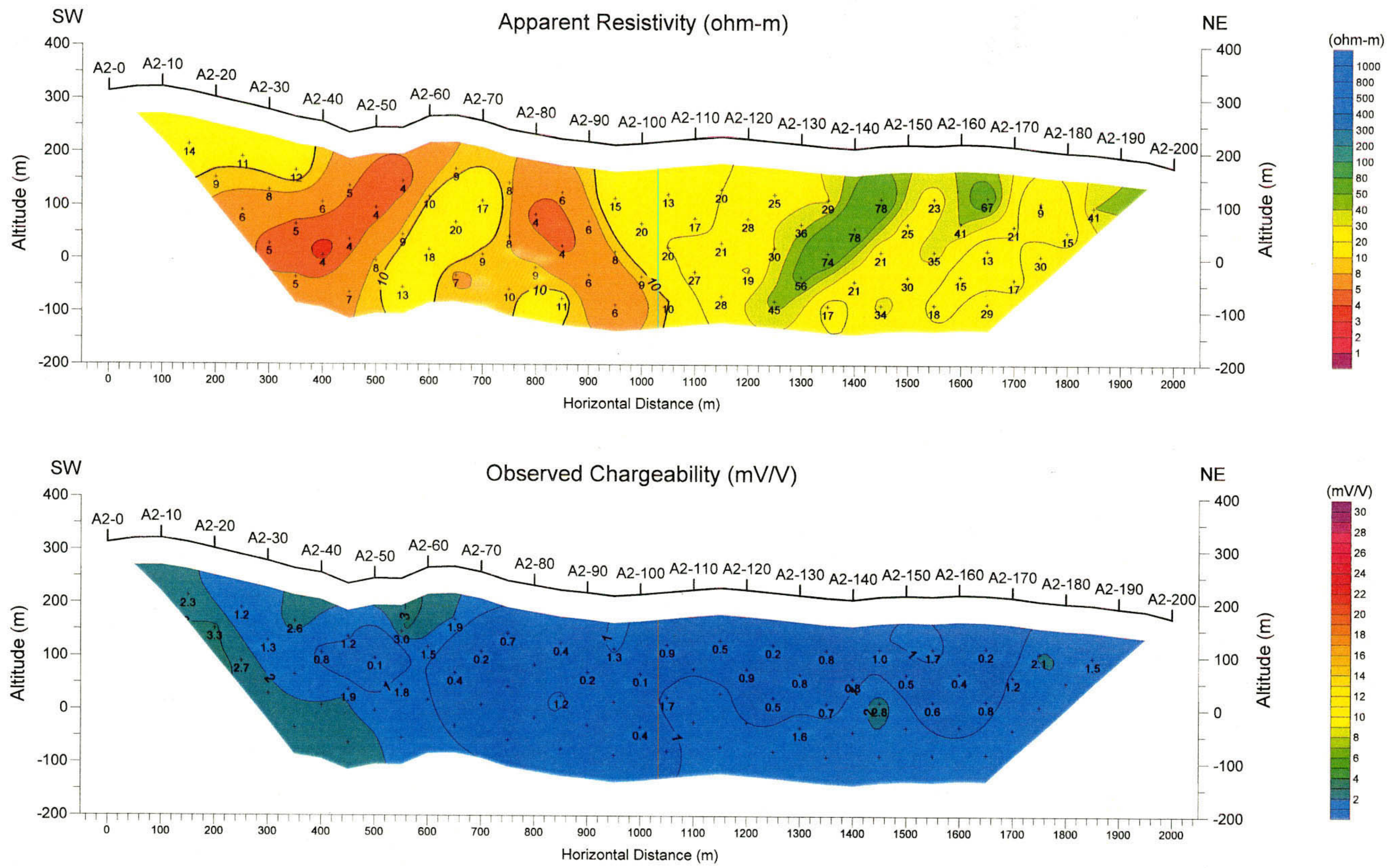

Figure 94 Observed IP pseudo-section (Line A2)

A1 from the southwest to the northeast. The apparent resistivity is generally less than 50 Ωm in the entire cross section. Low apparent resistivity anomaly less than 10 Ωm indicates the typical IP anomaly pattern "Λ", and the high apparent resistivity exceeding 50 Ωm extends at the shallow depth of the stations between A2-140 and A2-160 in the northeastern parts of the cross section.

The significant chargeability anomaly can not be also recognized in this cross section.

・Cross Section A3 (Figure 95)

This section runs in the NE-SW direction at 500 m to the southeast of the cross section A2. Low apparent resistivity anomalies less than 10 Ωm are widely distributed in the southwestern side from the vicinity of the station A3-60 and at depth of the stations between A3-80 and A3-90. Extensive high apparent resistivity anomalies are distributed at the shallow depth of the stations between A3-70 and A3-110 in the central parts and at depth of the stations between A3-120 and A3-140.

A weak measured chargeability anomalies are detected at the shallow depth of the station between A3-25 and A3-65 in the southwesternparts of the cross section, however those are not significant indications because of an one point anomaly within the low apparent resistivity anomaly.

・Cross Section A4 (Figure 96)

This section runs in NE-SW direction through the Mahjobia deposit in the central parts of the prospect. Low apparent resistivity less than 20Ωm is widely distributed for the entire cross section and the high apparent resistivity anomaly is not recognized. Low apparent resistivity anomalies less than 10 Ωm are distributed at the vicinity of the stations A4-100 in the central parts and A4-170 in the northeastern parts.

The significant measured chargeability anomaly is not detected over the Mahjobia working.

・Cross Section A5 (Figure 97)

This section runs in the NE-SW direction at 500 m to the southeast of the cross section A4. Low apparent resistivity less than 20 Ωm are dominated in the entire cross section and the low apparent resistivity anomaly less than 10Ωm extends also to the entire cross section.

A weak measured chargeability anomaly exceeding 4mV/V is detected at depth around the station A6-65 in the central parts of the cross section. However, this is also not significant indication because of one point anomaly within the low apparent resistivity anomaly.

・Cross Section A6 (Figure 98)

This section crosscuts the plain area at 500m to the southeast of the cross section A1 from southwest to northeast. Low apparent resistivity less than 20 Ωm are dominated in the entire

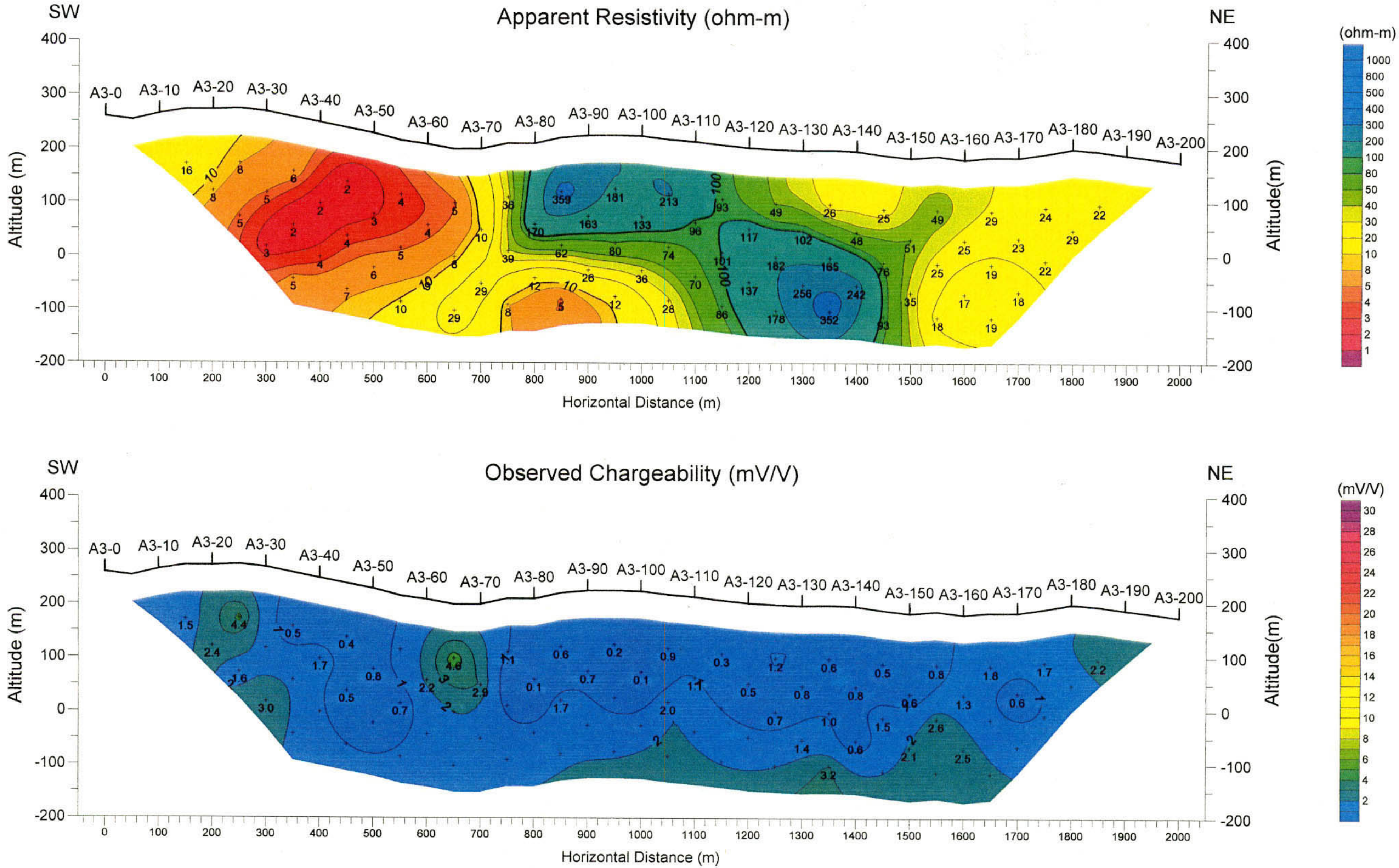

Figure 95 Observed IP pseudo-section (Line A3)

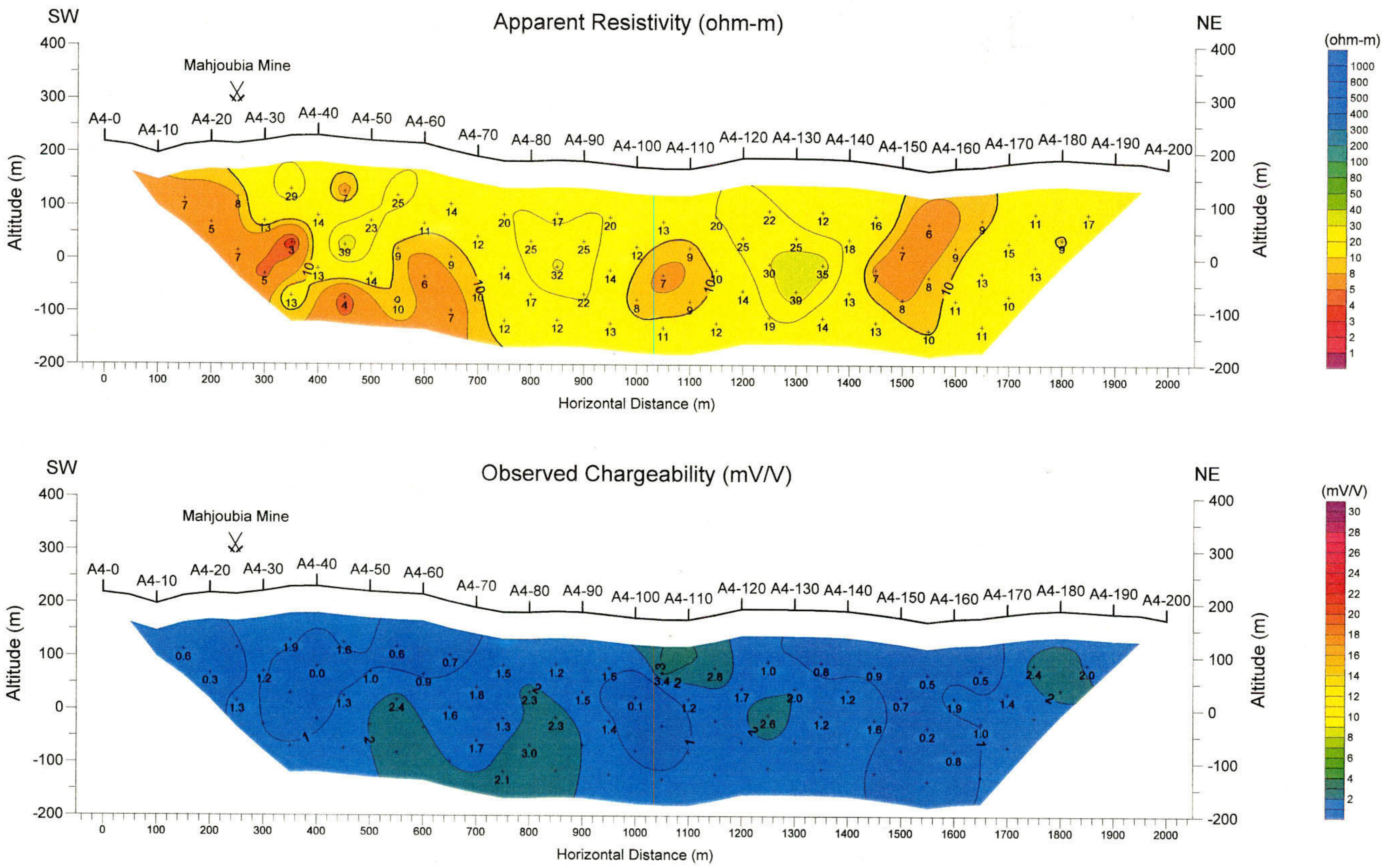

Figure 96 Observed IP pseudo-section (Line A4)

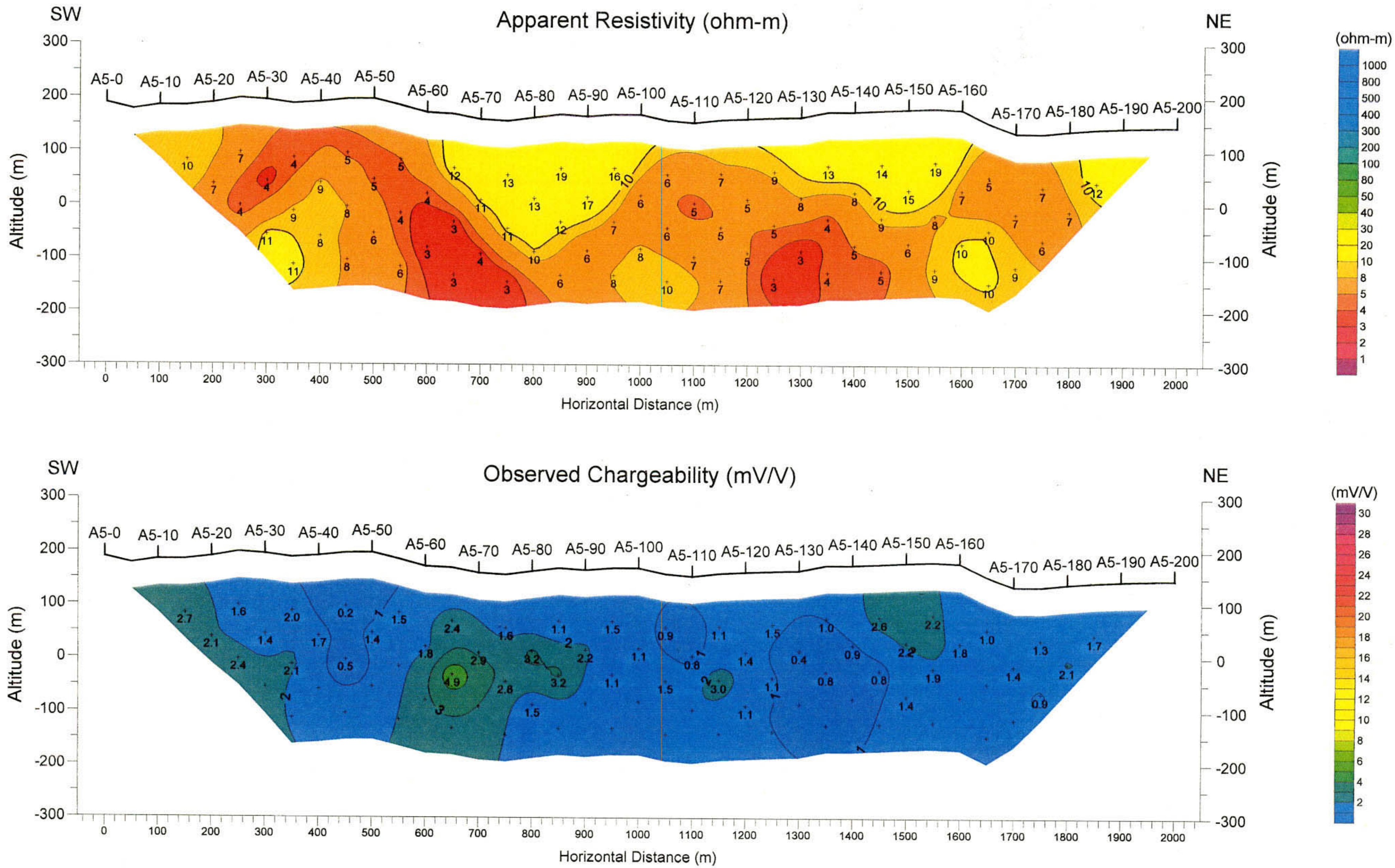

Figure 97 Observed IP pseudo-section (Line A5)

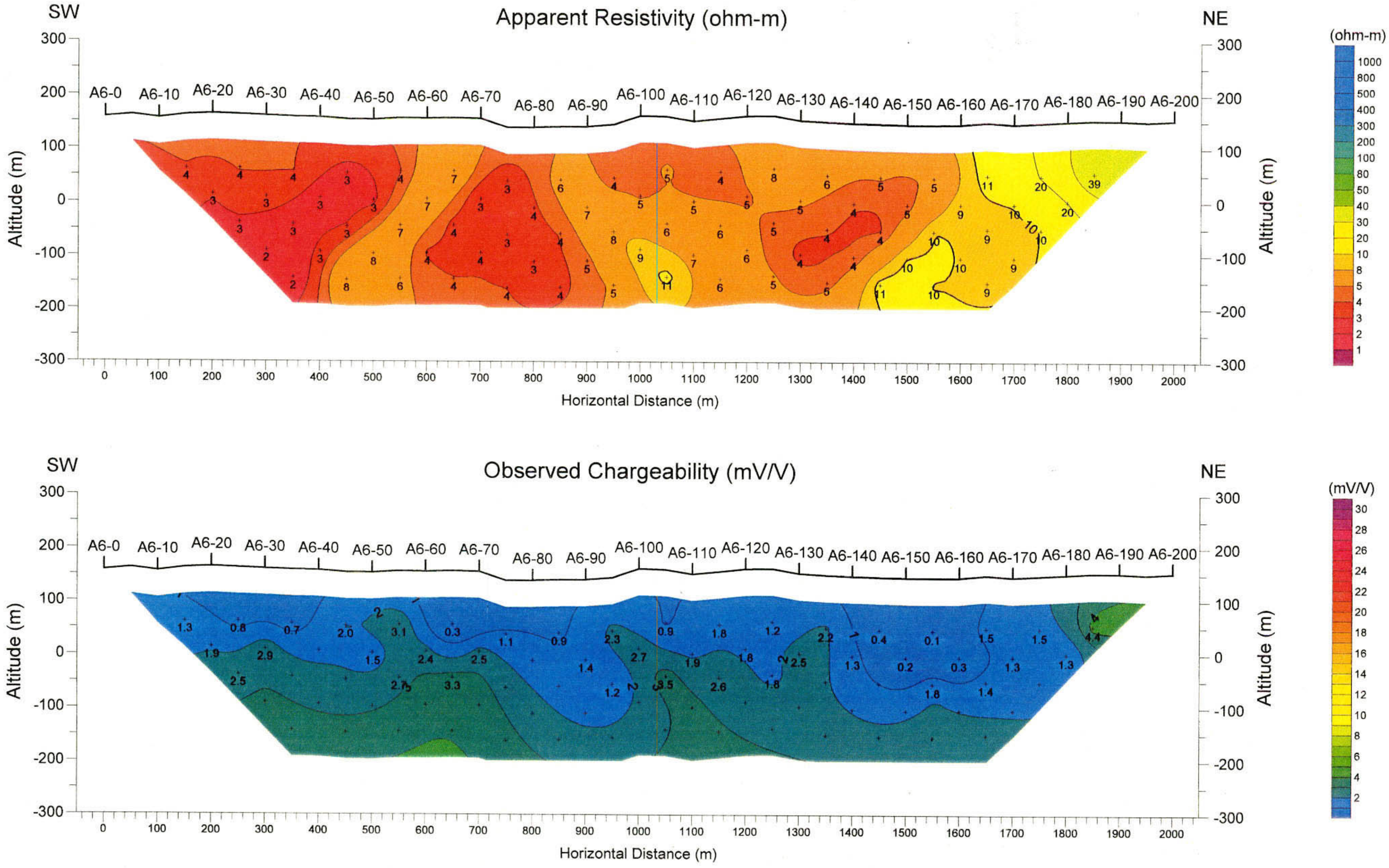

Figure 98 Observed IP pseudo-section (Line A6)

cross section and the low apparent resistivity anomaly less than 10 Ωm extends also to the entire cross section.

A weak measured chargeability anomaly exceeding 4mV/V is detected at depth of the station around A5-65 in the central parts of the cross section. However this is also not significant indication because of one point anomaly within the low apparent resistivity anomaly.

・Cross Section A7 (Figure 99)

This section crosscuts the plain area in the southeast parts of the prospect from southwest to northeast. The low apparent resistivity anomaly less than 10 Ωm extends to the southwestern half of the cross section and the relatively high zone with the apparent resistivity ranging from 30 to 60 Ωm extends to the northeastern half of the cross section. The former low resistivity anomaly is correlated to the margin of the El Aroussa plain covered by the unconsolidated layer of the Tertiary system.

A weak measured chargeability anomaly exceeding 4mV/V is detected at shallow depth of around the station A7-125 in the central parts of the cross section

・Plan map of apparent resistivity n=1 (Figure 100)

The zone of the low apparent resistivity less than 10 Ωm extending towards the WNW-ESE direction is distributed in the southeastern and southern parts of the prospect. The narrow anomaly zone of the low apparent resistivity less than 10 Ωm is stretching out towards the station A1-120 in the northwest direction from the station A4-0 in the western side of the former low zone. The zone of the low apparent resistivity in the southern parts is jutting out towards northeast from the station A0-260 in the northern parts and the extremity of the jut is bending towards the station A4-165 from the vicinity of the station A5-170. Small high apparent resistivity anomaly exceeding 100 Ωm is distributed in the vicinity of the station A0-140 in the central parts of the prospect and extends towards north. The high apparent resistivity anomalies exceeding 40 Ωm are distributed covering the stations A7-120 and A6-200 in the eastern parts of the prospect.

・Plan map of apparent resistivity n=2 (Figure101)

The distribution pattern of the apparent resistivity is similar to that of the previous plan n=1. The zone of the low apparent resistivity less than 10 Ωm extending from the central parts to the southern parts of the prospect becomes wider compare with that of the plan n=1. Especially, the narrow stretching out of the low apparent resistivity anomaly observed in the western parts becomes wider and combines with the zone of the low apparent resistivity extending in the southern parts. Small high apparent resistivity anomaly exceeding 100 Ωm

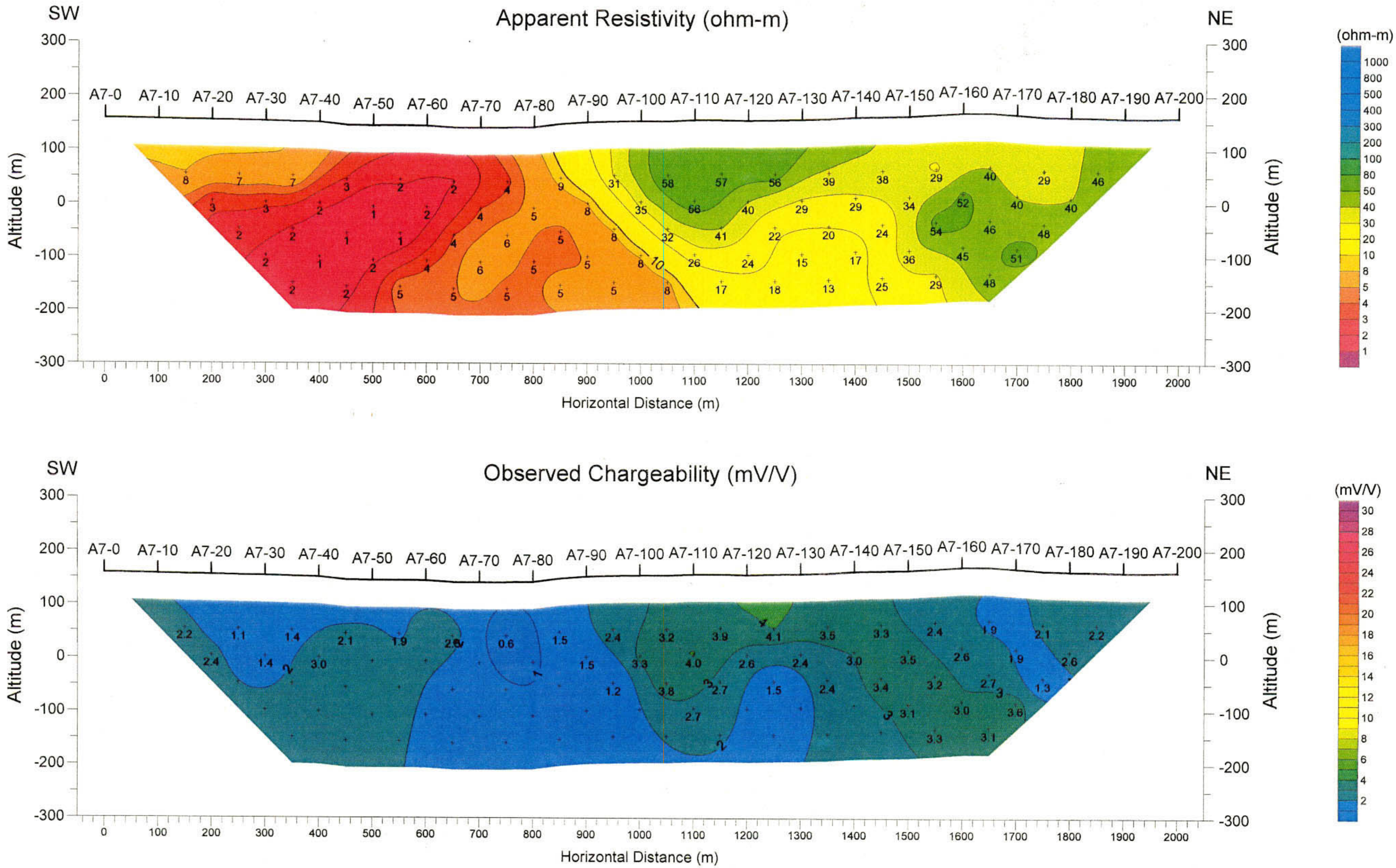

Figure 99 Observed IP pseudo-section (Line A7)

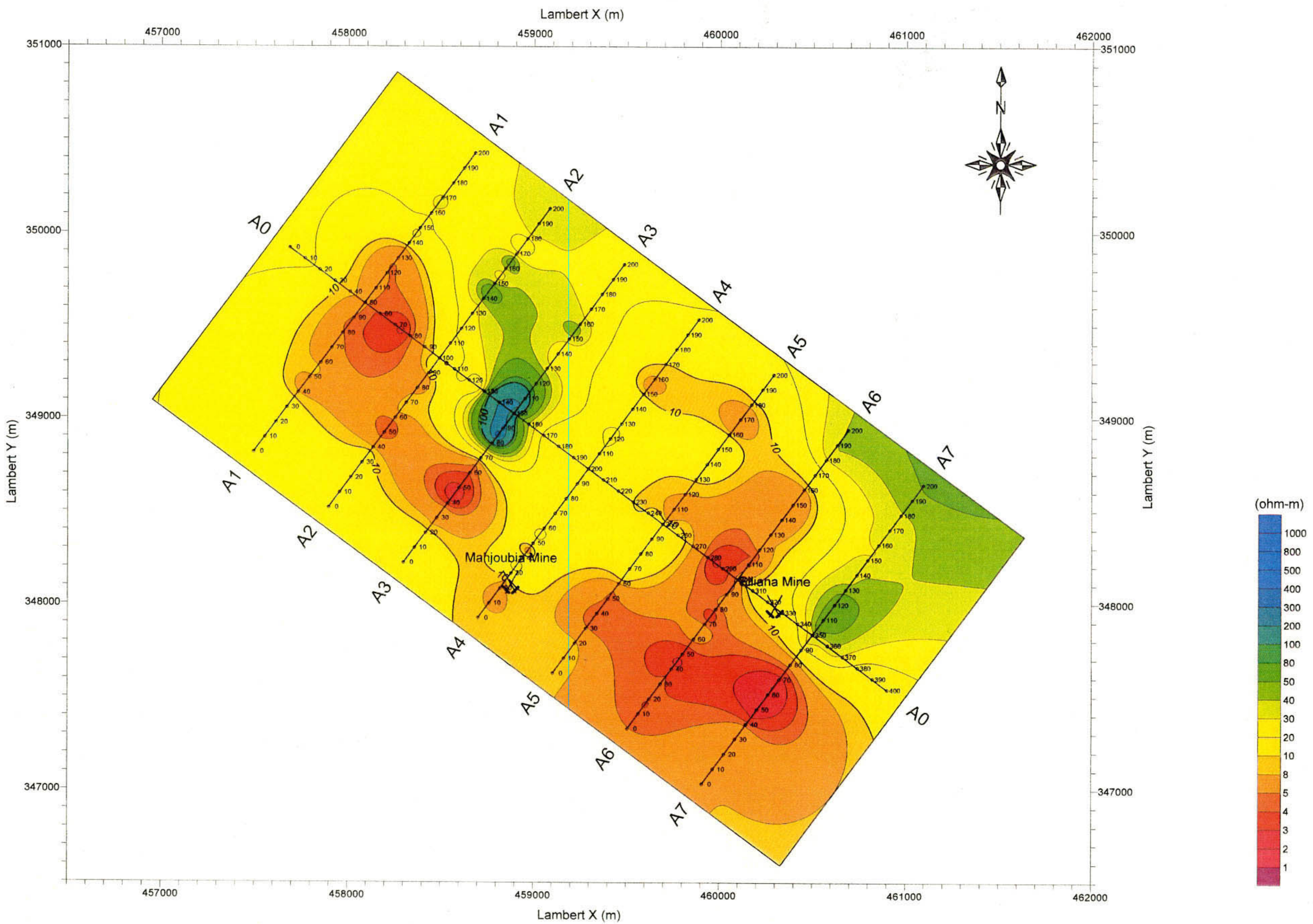

Figure 100 Plan map of apparent resistivity in Siliana prospect (n=1)

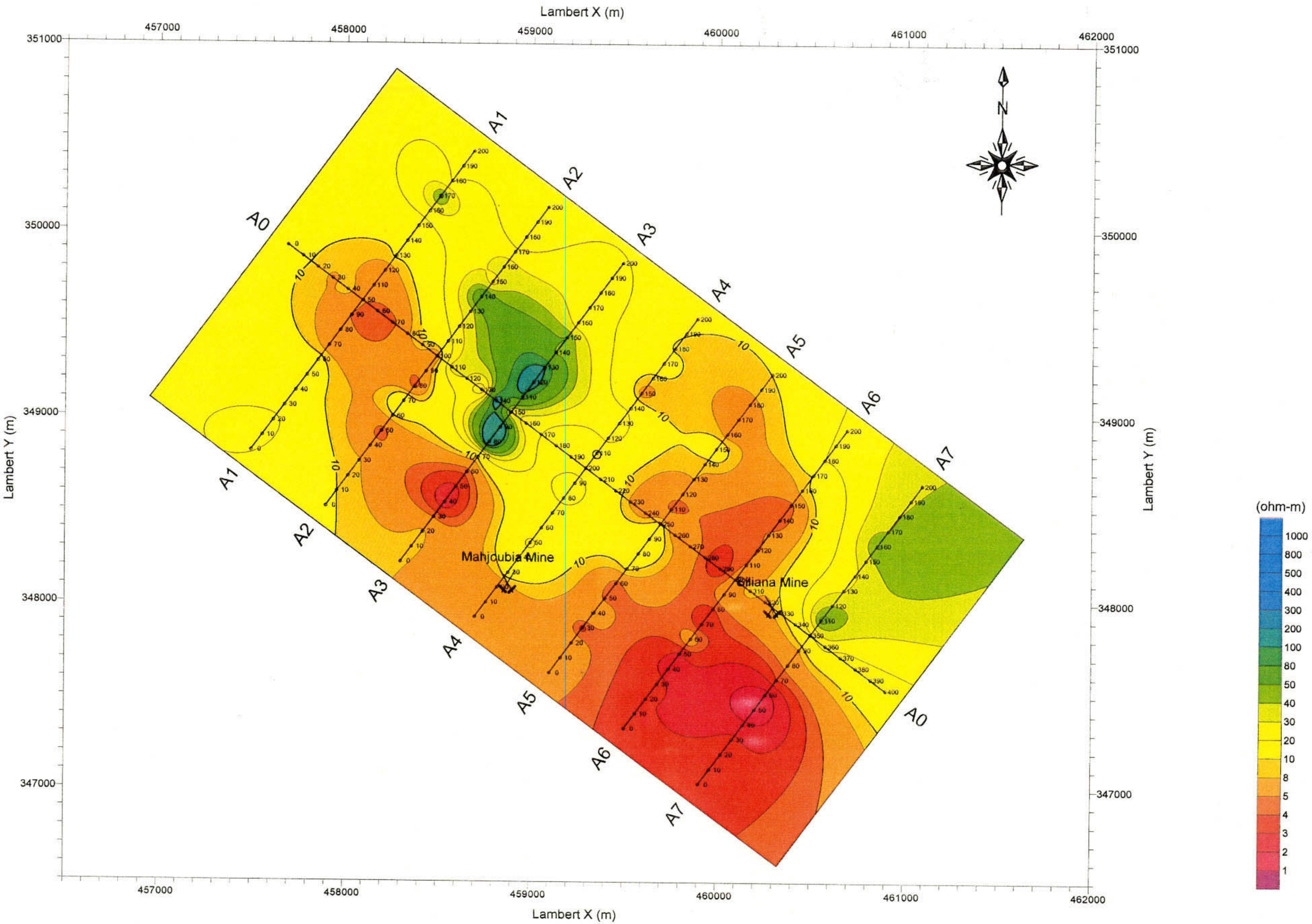

Figure 101 Plan map of apparent resistivity in Siliana prospect (n=2)